Using e^+e^- and $\gamma\gamma$ Collisions to Probe the Scalar Sector of the Randall-Sundrum Model

Jack Gunion
Davis Institute for High Energy Physics, U.C. Davis

Collaborators: D. Dominici, B. Grzadkowski, M. Toharia

Brief summary of updates on this and other topics:
New results for a photon-photon collider
D. Asner, B. Grzadkowski, J.F. Gunion
H.E. Logan, V. Martin, M. Schmitt, M.M. Velasco, hep-ph/0208219.

LCWS, Jeju, Korea, August 27, 2002

Outline

- **Understanding the parameter space**
- **Basics of the couplings**
- **Phenomenology**
- **Conclusions**

Presuming the new physics scale to be close to the TeV scale, there can be a rich new phenomenology in which Higgs and radion physics intermingle if the $\xi R \widehat{H}^\dagger \widehat{H}$ mixing term is present in $\mathcal{L}$.

Reference:

- **D. Dominici, B. Grzadkowski, J. F. Gunion and M. Toharia, "The scalar sector of the Randall-Sundrum model," arXiv:hep-ph/0206192.**

Previous work:

- $\xi = 0$:

1. S. B. Bae, P. Ko, H. S. Lee and J. Lee, Phys. Lett. B 487, 299 (2000) [arXiv:hep-ph/0002224].
2. H. Davoudiasl, J. L. Hewett and T. G. Rizzo, Phys. Rev. Lett. 84, 2080 (2000) [arXiv:hep-ph/9909255].
3. K. Cheung, Phys. Rev. D 63, 056007 (2001) [arXiv:hep-ph/0009232].
4. H. Davoudiasl, J. L. Hewett and T. G. Rizzo, Phys. Rev. D 63, 075004 (2001) [arXiv:hep-ph/0006041].
5. S. C. Park, H. S. Song and J. Song, Phys. Rev. D 63, 077701 (2001) [arXiv:hep-ph/0009245].

- $\xi \neq 0$:

1. G. Giudice, R. Rattazzi, J. Wells, Nucl. Phys. B595 (2001), 250, hep-ph/0002178.
2. C. Csaki, M.L. Graesser, G.D. Kribs, Phys. Rev. D63 (2001), 065002-1, hep-th/0008151.
3. T. Han, G. D. Kribs and B. McElrath, Phys. Rev. D 64, 076003 (2001) [arXiv:hep-ph/0104074].

4. M. Chaichian, A. Datta, K. Huitu and Z. h. Yu, Phys. Lett. B 524, 161 (2002) [arXiv:hep-ph/0110035].
5. J. L. Hewett and T. G. Rizzo, hep-ph/0202155.
6. C. Csaki, M. Graesser, L. Randall and J. Terning, Phys. Rev. D 62, 045015 (2000) [arXiv:hep-ph/9911406].

Randal-Sundrum Review

Some possibly very dramatic changes in phenomenology.

- There are two branes, separated in the 5th dimension (y) and $y \to -y$ symmetry is imposed. With appropriate boundary conditions, the 5D Einstein equations $\Rightarrow$

$$ds^2 = e^{-2\sigma(y)} \eta_{\mu\nu} dx^\mu dx^\nu - b_0^2 dy^2, \tag{1}$$

  where $\sigma(y) \sim m_0 b_0 |y|$.

- $e^{-2\sigma(y)}$ is the warp factor; scales at $y = 0$ of order M_{Pl} on the hidden brane are reduced to scales at $y = 1/2$ of order TeV on the visible brane.

- Fluctuations of $g_{\mu\nu}$ relative to $\eta_{\mu\nu}$ are the KK excitations $h^n_{\mu\nu}$.

- Fluctuations of $b(x)$ relative to b_0 define the radion field.

- In addition, we place a Higgs doublet $\widehat{H}$ on the visible brane.

Including the ξ mixing term

- **We begin with**

$$S_{\xi} = \xi \int d^4x \sqrt{g_{\mathrm{vis}}} R(g_{\mathrm{vis}}) \widehat{H}^{\dagger} \widehat{H} \,, \tag{2}$$

where $R(g_{\mathrm{vis}})$ is the Ricci scalar for the metric induced on the visible brane.

- **A crucial parameter is the ratio**

$$\gamma \equiv v_0 / \Lambda_{\phi} \,. \tag{3}$$

where Λ_{ϕ} is vacuum expectation value of the radion field.

- **After writing out the full quadratic structure of the Lagrangian, including $\xi \neq 0$ mixing, we obtain a form in which the h_0 and ϕ_0 fields for $\xi = 0$ are mixed and have complicated kinetic energy normalization.**

  We must diagonalize the kinetic energy and rescale to get canonical

normalization.

$$
\begin{aligned}
h_0 &= \left(\cos\theta - \frac{6\xi\gamma}{Z}\sin\theta\right) h + \left(\sin\theta + \frac{6\xi\gamma}{Z}\cos\theta\right)\phi \\
&\equiv dh + c\phi \qquad (4) \\
\phi_0 &= -\cos\theta\frac{\phi}{Z} + \sin\theta\frac{h}{Z} \equiv a\phi + bh\,. \qquad (5)
\end{aligned}
$$

- In the above equations

$$
Z^2 \equiv 1 + 6\xi\gamma^2(1-6\xi)\,. \qquad (6)
$$

$Z^2 > 0$ is required to avoid tachyonic situation.

This $\Rightarrow$ constraint on maximum neg. and pos. ξ values:

$$
\frac{1}{12}\left(1-\sqrt{1+\frac{4}{\gamma^2}}\right) \leq \xi \leq \frac{1}{12}\left(1+\sqrt{1+\frac{4}{\gamma^2}}\right) \qquad (7)
$$

- **The corresponding mass-squared eigenvalues are**

$$m_\pm^2 = \frac{1}{2Z^2}\left(m_{\phi_0}^2 + \beta m_{h_0}^2 \pm \left\{[m_{\phi_0}^2 + \beta m_{h_0}^2]^2 - 4Z^2 m_{\phi_0}^2 m_{h_0}^2\right\}^{1/2}\right), \tag{8}$$

with $\beta \equiv 1 + 6\xi\gamma^2$ **and** $\mathrm{Max}[m_h, m_\phi] = m_+$.

- **The process of inversion is very critical to the phenomenology and somewhat delicate.**

- **One finds:**

$$[\beta m_{h_0}^2, m_{\phi_0}^2] = \frac{Z^2}{2}\left[m_+^2 + m_-^2 \pm \left\{(m_+^2 + m_-^2)^2 - \frac{4\beta m_+^2 m_-^2}{Z^2}\right\}^{1/2}\right]. \tag{9}$$

- **For the quantity inside the square root appearing in Eq. (9) to be positive, we require that:**

$$\frac{m_+^2}{m_-^2} > 1 + \frac{2\beta}{Z^2}\left(1 - \frac{Z^2}{\beta}\right) + \frac{2\beta}{Z^2}\left[1 - \frac{Z^2}{\beta}\right]^{1/2}, \tag{10}$$

where $1 - Z^2/\beta = 36\xi^2\gamma^2/\beta > 0$.

I.e. since we will identify m_+ with either m_h or m_ϕ, the physical states h and ϕ cannot be too close to being degenerate in mass, depending on the precise values of ξ and γ; extreme degeneracy is allowed only for small ξ and/or γ.

- A two-fold ambiguity remains in solving for $\beta m_{h_0}^2$ and $m_{\phi_0}^2$, corresponding to which we take to be the larger.

  We resolve this ambiguity by requiring that $m_{h_0}^2 \to m_h^2$ in the $\xi \to 0$ limit. This means that for $\beta m_{h_0}^2$ we take the $+$ ($-$) sign in Eq. (9) for $m_h > m_\phi$ ($m_h < m_\phi$), *i.e.* for $m_h = m_+$ ($m_h = m_-$), respectively.

- Given this choice, we complete the inversion by writing out the kinetic energy terms of the complete Lagrangian using the substitutions of Eqs. (4) and (5) and demanding that the coefficients of $-\frac{1}{2}h^2$ and $-\frac{1}{2}\phi^2$ agree with the given input values for m_h^2 and m_ϕ^2.

Using this inversion, for given ξ, γ, m_h and m_ϕ we compute Z^2, $m_{h_0}^2$ and $m_{\phi_0}^2$, θ to obtain a, b, c, d in Eqs. (4) and (5).

- **Net result**

4 independent parameters to completely fix the mass diagonalization of the scalar sector when $\xi \neq 0$. These are:

$$\xi\,, \quad \gamma\,, \quad m_h\,, \quad m_\phi\,, \tag{11}$$

where we recall that $\gamma \equiv v_0/\Lambda_\phi$ with $v_0 = 246~\mathrm{GeV}$.

Two additional parameters will be required to completely fix the phenomenology of the scalar sector, including all possible decays. These are

$$\widehat{\Lambda}_W\,, \quad m_1\,, \tag{12}$$

where $\widehat{\Lambda}_W$ will determine KK-graviton couplings to the h and ϕ and m_1 is the mass of the first KK graviton excitation.

There are relations among parameters:

$$\widehat{\Lambda}_W \simeq \sqrt{2} M_{Pl}\Omega_0\,, \quad m_n = m_0 x_n \Omega_0\,, \quad \Lambda_\phi = \sqrt{6} M_{Pl}\Omega_0 = \sqrt{3}\widehat{\Lambda}_W \tag{13}$$

where $\Omega_0 M_{Pl} = e^{-m_0 b_0/2} M_{Pl}$ should be of order a TeV to solve the hierarchy problem. In Eq. (13), the x_n are the zeroes of the Bessel function

J_1 ($x_1 \sim 3.8$, $x_2 \sim 7.0$). A useful relation following from the above equations is:

$$m_1 = x_1 \frac{m_0}{M_{Pl}} \frac{\Lambda_\phi}{\sqrt{6}} . \tag{14}$$

m_0/M_{Pl} is related to the curvature of the brane and should be a relatively small number for consistency of the RS scenario.

- Sample parameters that are safe from precision EW data and RunI Tevatron constraints are $\Lambda_\phi = 5~\mathrm{TeV}$ ($\Rightarrow \widehat{\Lambda}_W \sim 3~\mathrm{TeV}$) and $m_0/M_{Pl} = 0.1$.

  The latter $\Rightarrow m_1 \sim 780~\mathrm{GeV}$; i.e. m_1 is typically too large for KK graviton excitations to be present, or if present, important, in h, ϕ decays.

  Results shown take $m_0/M_{Pl} = 0.1$.

The Couplings

The $f\overline{f}$ and VV couplings

- **The VV couplings**
  - The h_0 has standard ZZ coupling.
  - The ϕ_0 has ZZ coupling deriving from the interaction $-\frac{\phi_0}{\Lambda_\phi}T^\mu_\mu$ using the covariant derivative portions of $T^\mu_\mu(h_0)$.

  The result for the $\eta_{\mu\nu}$ portion of the ZZ couplings is:

$$g_{ZZh} = \frac{g\, m_Z}{c_W}(d + \gamma b)\ , \quad g_{ZZ\phi} = \frac{g\, m_Z}{c_W}(c + \gamma a)\ . \tag{15}$$

  g and c_W denote the $SU(2)$ gauge coupling and $\cos\theta_W$, respectively. The WW couplings are obtained by replacing gm_Z/c_W by gm_W.

- **The $f\overline{f}$ couplings**
  - The h_0 has standard fermionic couplings.

– The fermionic couplings of the ϕ_0 derive from $-\frac{\phi_0}{\Lambda_\phi}T^\mu_\mu$ using the Yukawa interaction contributions to T^μ_μ.
– One obtains results in close analogy to the VV couplings just considered:

$$g_{f\bar{f}h} = -\frac{g\, m_f}{2\, m_W}(d+\gamma b)\,, \quad g_{f\bar{f}\phi} = -\frac{g\, m_f}{2\, m_W}(c+\gamma a)\,. \tag{16}$$

- Note same factors for WW and $f\bar{f}$ couplings.

  We define

$$g_{fVh} \equiv d+\gamma b; \quad g_{fV\phi} \equiv c+\gamma a; \tag{17}$$

- There is a sum rule:

$$g^2_{fVh} + g^2_{fV\phi} = R^2\,; \quad R^2 = 1 + \frac{\gamma^2(1-6\xi)^2}{Z^2} \tag{18}$$

  which says that $g^2_{fV\phi}$ must be at least as large as $1 - g^2_{fVh}$.

  R^2 can't be too large without problems with precision electroweak, but it can certainly be somewhat larger than 1.

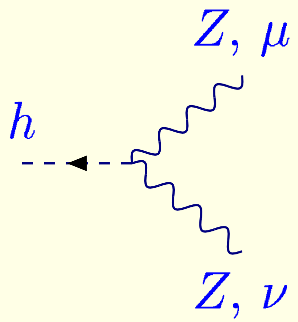

$$i\frac{g m_Z}{c_W}(d+\gamma b)\eta^{\mu\nu}$$

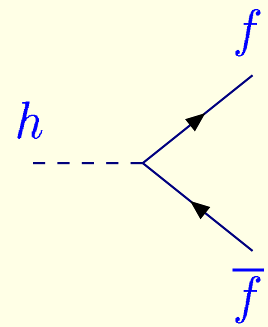

$$-i\frac{g}{2}\frac{m_f}{m_W}(d+\gamma b)$$

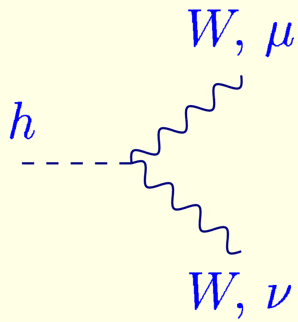

$$i g m_W(d+\gamma b)\eta^{\mu\nu}$$

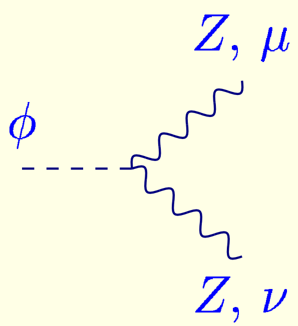

$$i\frac{g m_Z}{c_W}(c+\gamma a)\eta^{\mu\nu}$$

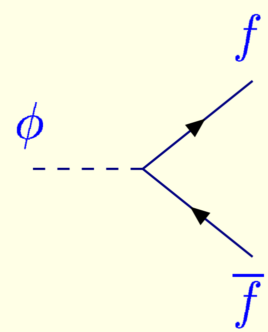

$$-i\frac{g}{2}\frac{m_f}{m_W}(c+\gamma a)$$

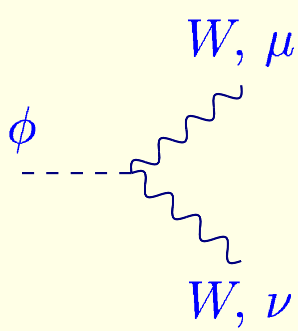

$$i g m_W(c+\gamma a)\eta^{\mu\nu}$$

The gg and $\gamma\gamma$ couplings

- There are the standard loop contributions, except rescaled by $f\overline{f}/VV$ strength factors g_{fVh} or $g_{fV\phi}$.

- In addition, there are anomalous contributions, which are expressed in terms of the SU(3)×SU(2)×U(1) β function coefficients $b_3 = 7$, $b_2 = 19/6$ and $b_Y = -41/6$.

- The anomalous couplings of h and ϕ enter only through their radion admixtures, $g_h = \gamma b$ for the h, and $g_\phi = \gamma a$ for the ϕ.

- **A VERY CRUCIAL POINT**

  All h couplings (other than self coupling) are determined by just the two combinations $g_{fVh} = (d + \gamma b)$ and $g_h = \gamma b$.

  Thus, if we imagine measuring g_{fVh} very precisely in $e^+e^- \to Zh$ inclusive, for example, we would wish to focus all other h measurements on determining γb.

Some measurements are very sensitive, and others are not.

Measurements of m_h, g_{fVh} impose 2 constraints on the four fundamental parameters, which can be viewed as m_h, m_ϕ, $\gamma\xi$, and γ. $\Rightarrow$ there will be a continuum of solutions.

To get a unique set of parameters requires more observations. For example, one might

– Measure m_ϕ and $g_{fV\phi}$ directly by observing the ϕ in $e^+e^- \to Z\phi$.

But, the ϕ will not always be directly observable.

$Zh\phi$ tree level couplings are absent.

The cubic interactions

- There are four major sources of cubic interactions involving the h, the ϕ and the KK gravitons.

- For $\xi \neq 0$, they can lead to $h \to \phi\phi$ decays or the reverse $\phi \to hh$ decays.

  The $h \to \phi\phi$ decays typically have small BR for light h.

  $BR(\phi \to hh)$ can be substantial if the ϕ is heavy.

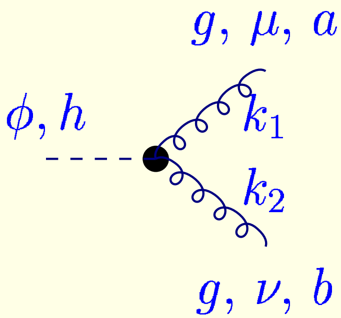

$$ic_g\delta^{ab}[k_1\cdot k_2\eta^{\mu\nu}-k_1^\nu k_2^\mu]:\ c_g=-\tfrac{\alpha_s}{4\pi v}[g_{fV}\textstyle\sum_i F_{1/2}(\tau_i)-2b_3g_r]$$

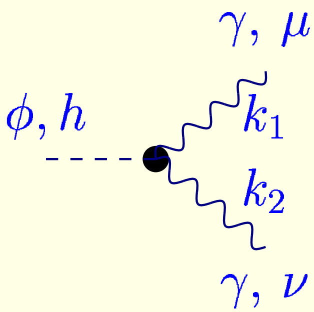

$$ic_\gamma[k_1\cdot k_2\eta^{\mu\nu}-k_1^\nu k_2^\mu]:\ c_\gamma=-\tfrac{\alpha}{2\pi v}[g_{fV}\textstyle\sum_i e_i^2N_c^iF_i(\tau_i)-(b_2+b_Y)g_r]$$

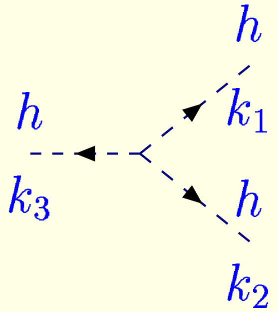

$$i\frac{g_{hhh}}{\Lambda_\phi} \equiv \frac{i}{\Lambda_\phi}\left[bd\left\{[12b\gamma\xi + d(6\xi+1)]\left(k_1^2+k_2^2+k_3^2\right) - 12dm_{h_0}^2\right\} - 3\gamma^{-1}d^3m_{h_0}^2\right]$$

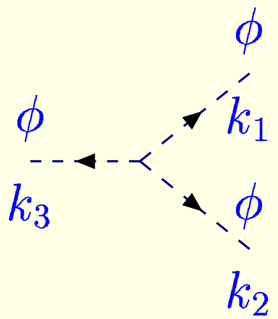

$$i\frac{g_{\phi\phi\phi}}{\Lambda_\phi} \equiv \frac{i}{\Lambda_\phi}\left[ac\left\{[12a\gamma\xi + c(6\xi+1)]\left(k_1^2+k_2^2+k_3^2\right) - 12cm_{h_0}^2\right\} - 3\gamma^{-1}c^3m_{h_0}^2\right]$$

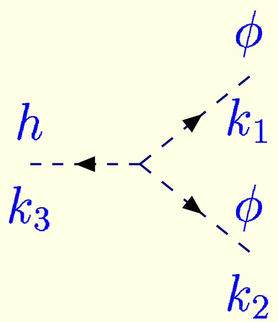

$$i\frac{g_{\phi\phi h}}{\Lambda_\phi} \equiv \frac{i}{\Lambda_\phi}\Big[\left\{6a\xi(\gamma(ad+bc)+cd)+bc^2\right\}(k_1^2+k_2^2) + c\left\{12ab\gamma\xi + 2ad + bc(6\xi-1)\right\}k_3^2 - 4c(2ad+bc)m_{h_0}^2 - 3\gamma^{-1}c^2dm_{h_0}^2\Big]$$

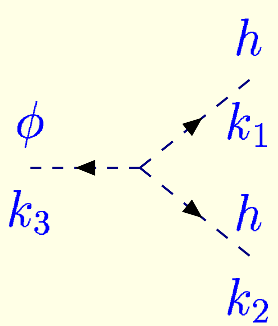

$$i\frac{g_{\phi hh}}{\Lambda_\phi} \equiv \frac{i}{\Lambda_\phi}\Big[\left\{6b\xi(\gamma(ad+bc)+cd)+ad^2\right\}(k_1^2+k_2^2) + d\left\{12ab\gamma\xi + 2bc + ad(6\xi-1)\right\}k_3^2 - 4d(ad+2bc)m_{h_0}^2 - 3\gamma^{-1}cd^2m_{h_0}^2\Big]$$

Constraints from LEP/LEP2

- **To illustrate, temporarily choose $\Lambda_\phi = 5$ TeV, i.e. $\gamma \sim 0.05$.**

  $Z^2 > 0$ gives ξ constraint.

  The mass difference $|m_h - m_\phi|$ increases with $|\xi|$ (because of requirement for successful inversion back to h_0, ϕ_0 basis).

  Exact results very sensitive to including all kinetic energy terms in the h_0, ϕ_0 basis.

- **LEP/LEP2 provides an upper limit on ZZs ($s = h$ or ϕ) from which we can exclude regions in the (m_h, m_ϕ) plane for a given choice of R^2.**

  Use upper limits on the ZZs coupling in both with and without b tagging, with computed branching ratios into b and non-b final states.

- **Conclusions:**

  Small m_ϕ relative to m_h is entirely possible given current data so long as $m_h \gtrsim 115$ GeV. (The $ZZ\phi$ coupling does not blow up.)

  $m_\phi > m_h$ is also possible, but to avoid conflict with precision electroweak data $g_{ZZ\phi}$ must not be too large if m_ϕ is large.

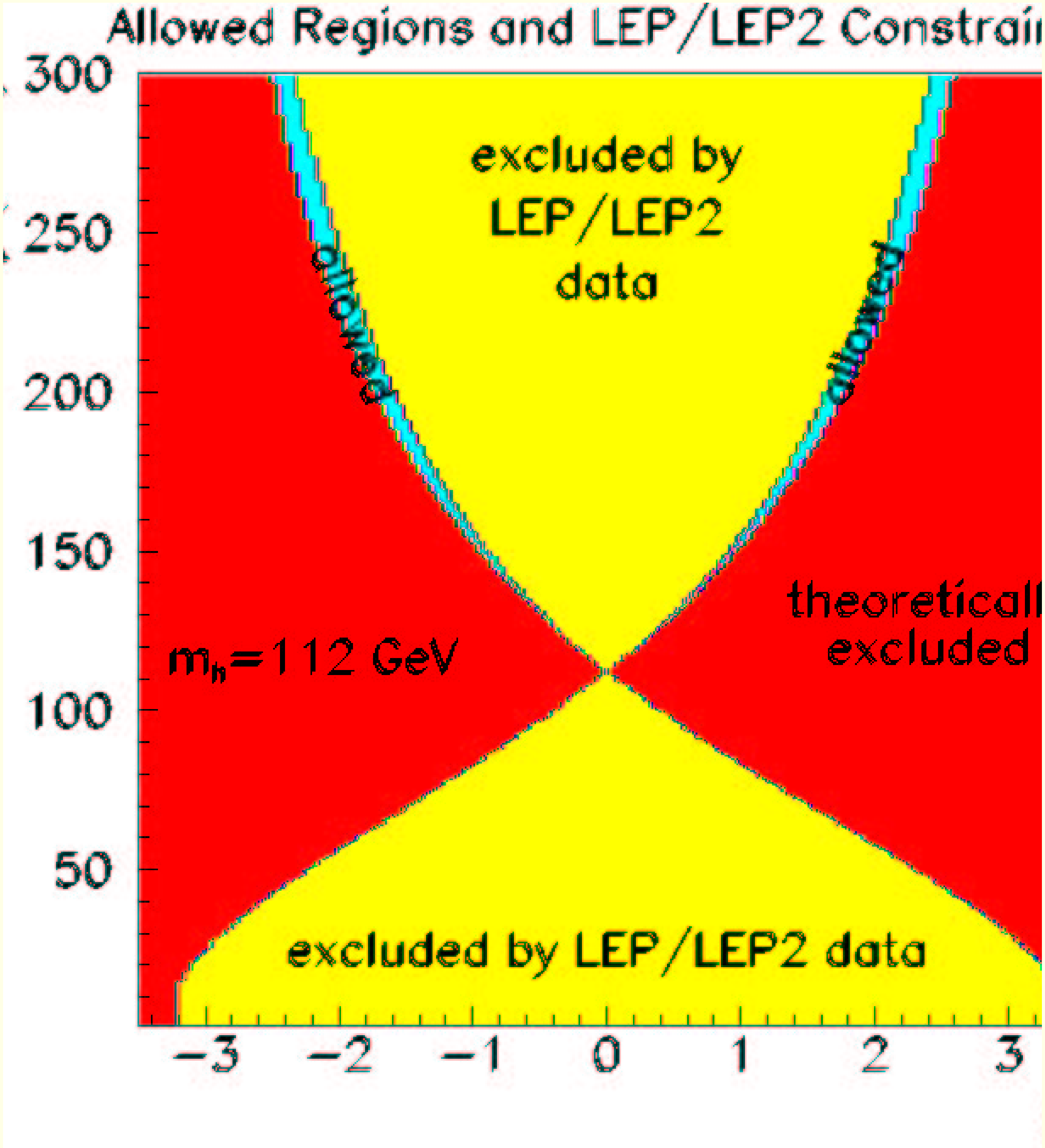
Allowed Regions and LEP/LEP2 Constrai
excluded by
LEP/LEP2
data
allowed
allowed
theoreticall
excluded
m_h=112 GeV
excluded by LEP/LEP2 data
300
250
200
150
100
50
−3
−2
−1
0
1
2
3

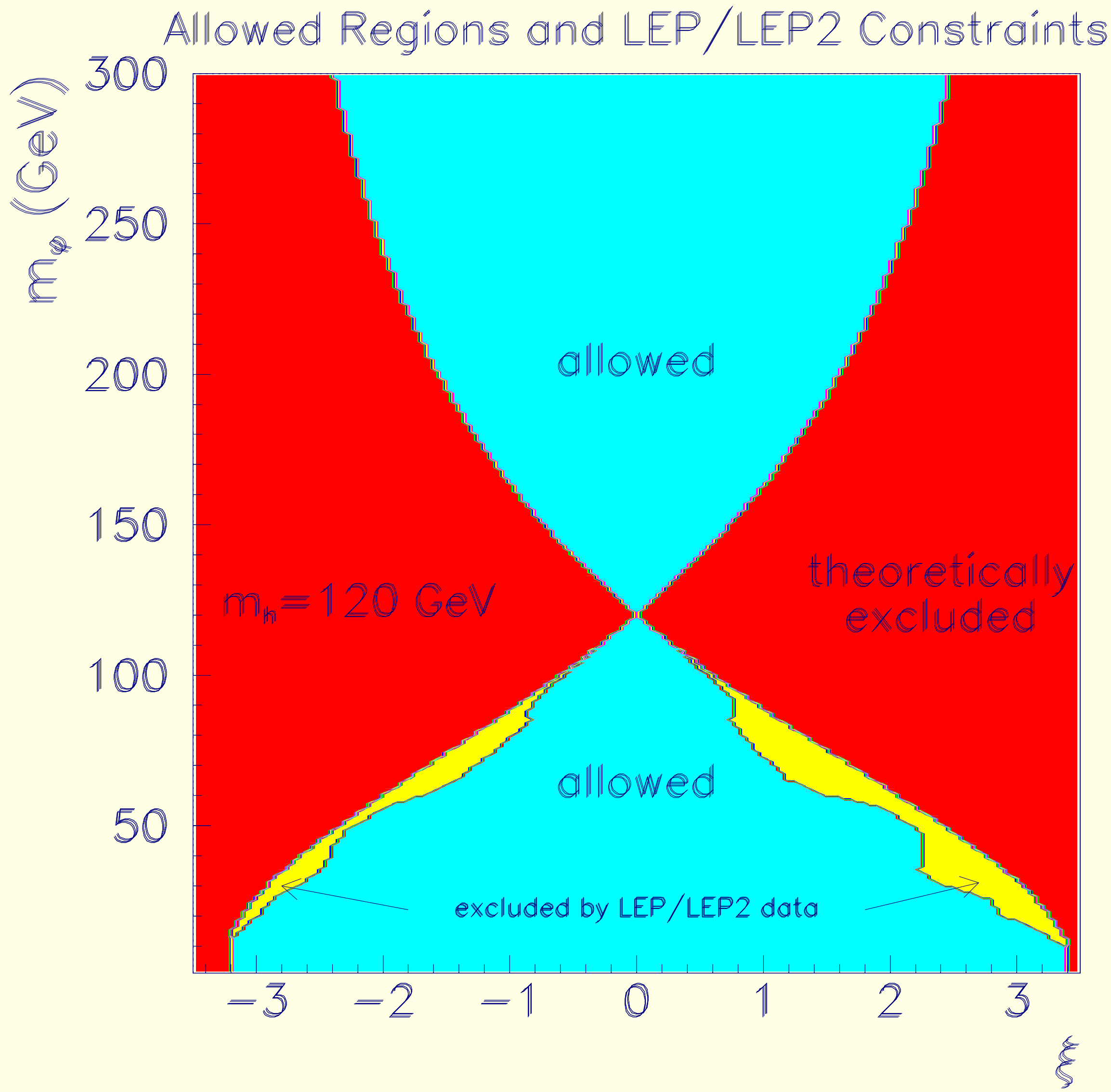

Allowed Regions and LEP/LEP2 Constraints
m_ϕ (GeV)
300
250
200
150
100
50
allowed
theoretically
excluded
m_h=120 GeV
allowed
excluded by LEP/LEP2 data
−3
−2
−1
0
1
2
3
ξ

Couplings

- First, consider the $f\overline{f}/VV$ couplings of h and ϕ relative to SM, taking $m_h = 120$ GeV and $\Lambda_\phi = 5$ TeV.

- $\boxed{\text{The most important point}}$

  After imposing LEP/LEP2 restrictions and bounds on Z^2 (precision EW), if $g^2_{fVh} < 1$ is observed then $m_\phi > m_h$, and vice versa, except for small region near $\xi = 0$.

  In cases where $g_{fV\phi}$ is small, prior indirect knowledge of, or constraints on, m_ϕ could be crucial.

- The cubic couplings are also of potential interest.
  - These display substantial variation.
    For the h, new physics would be abundantly apparent with even a relatively modest error on the measurement.
  - However, the ϕ^3 self coupling tends to be quite small and will be difficult to measure in much of parameter space.

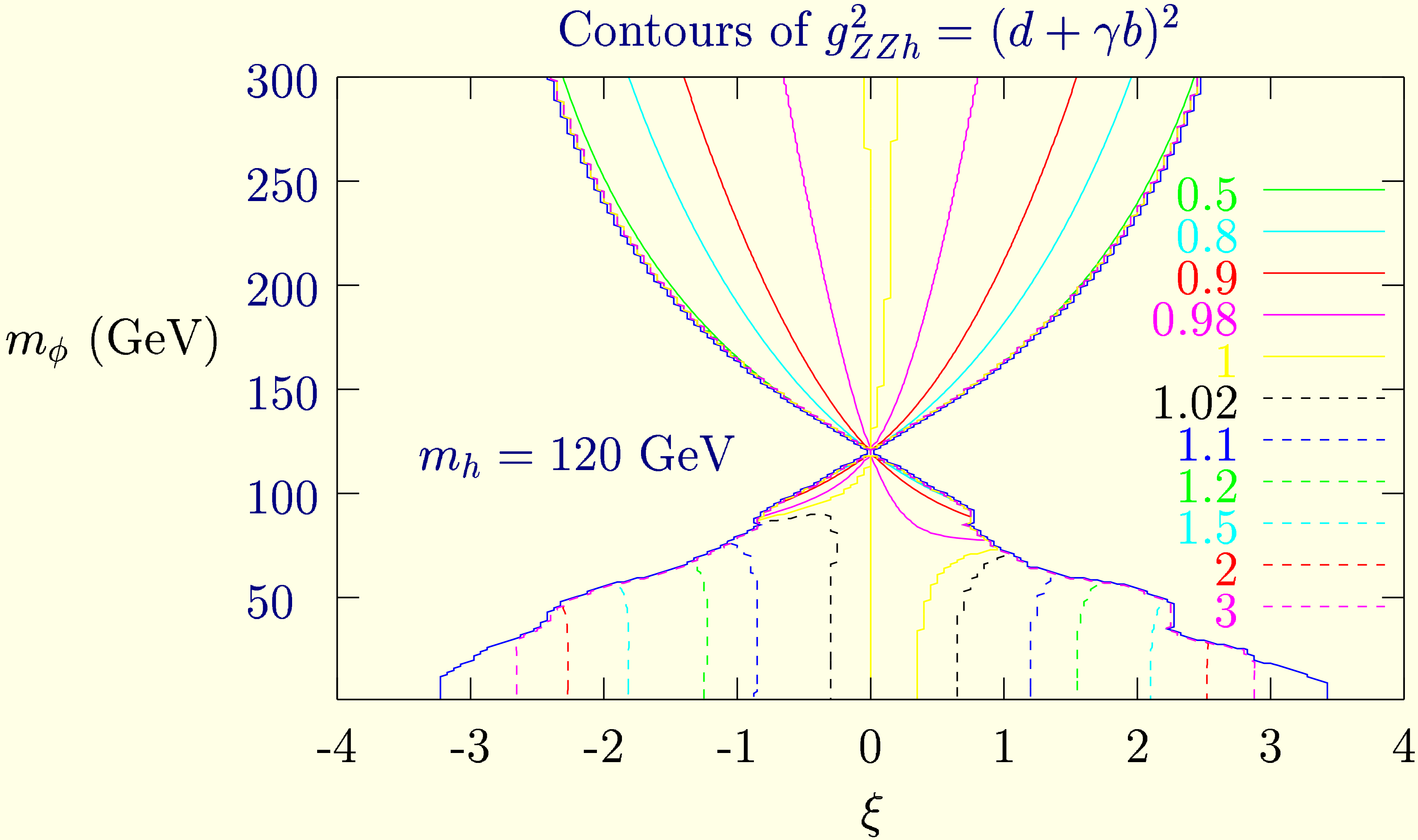

Figure 1: Contours of g^2_{fVh} for $\Lambda_\phi = 5$ TeV, $m_h = 120$ GeV

- **Observe suppression if $m_\phi > m_h$ and vice versa.**

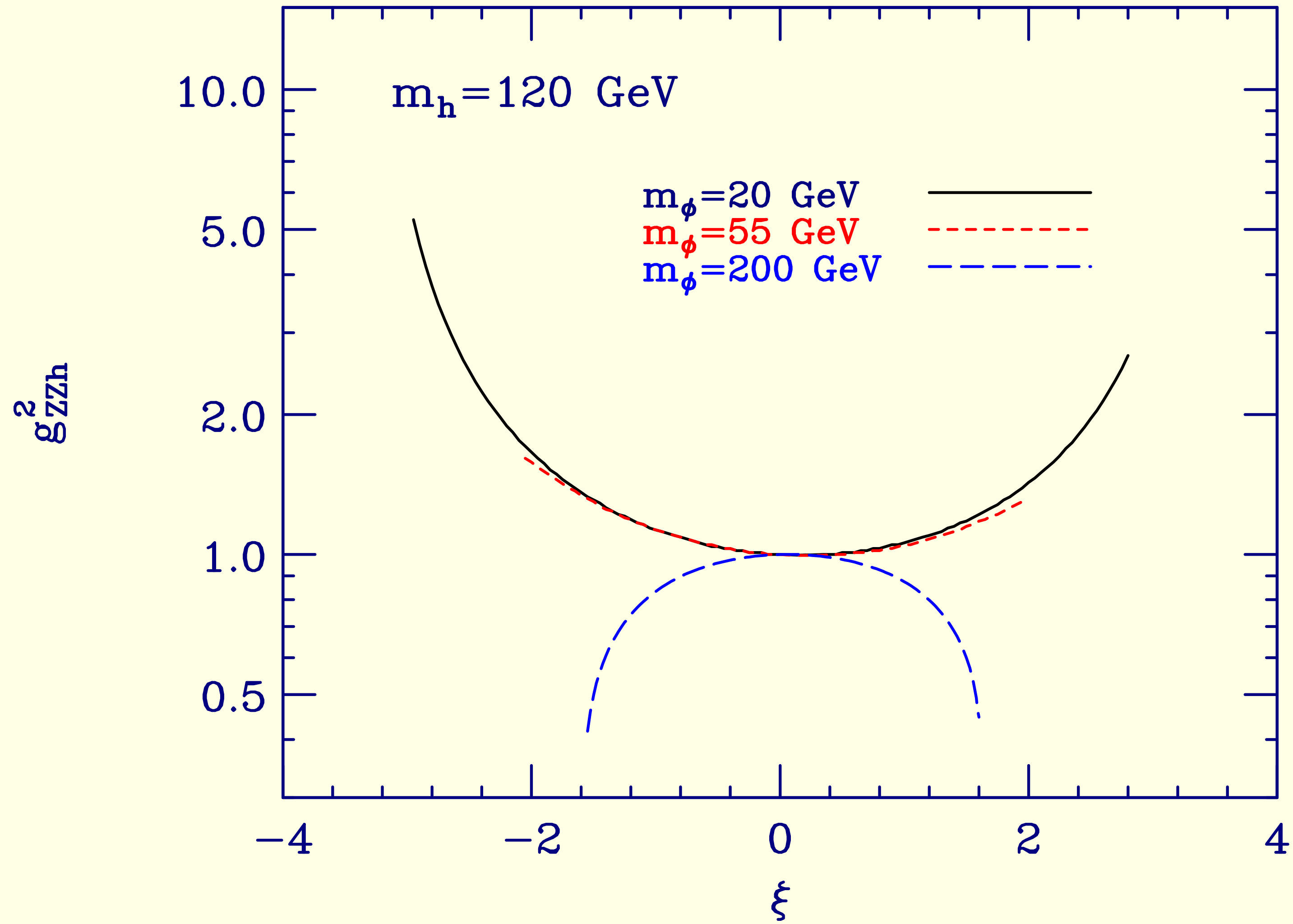

m_h=120 GeV
m_ϕ=20 GeV
m_ϕ=55 GeV
m_ϕ=200 GeV
10.0
5.0
2.0
1.0
0.5
g^2_{ZZh}
−4
−2
0
2
4
ξ

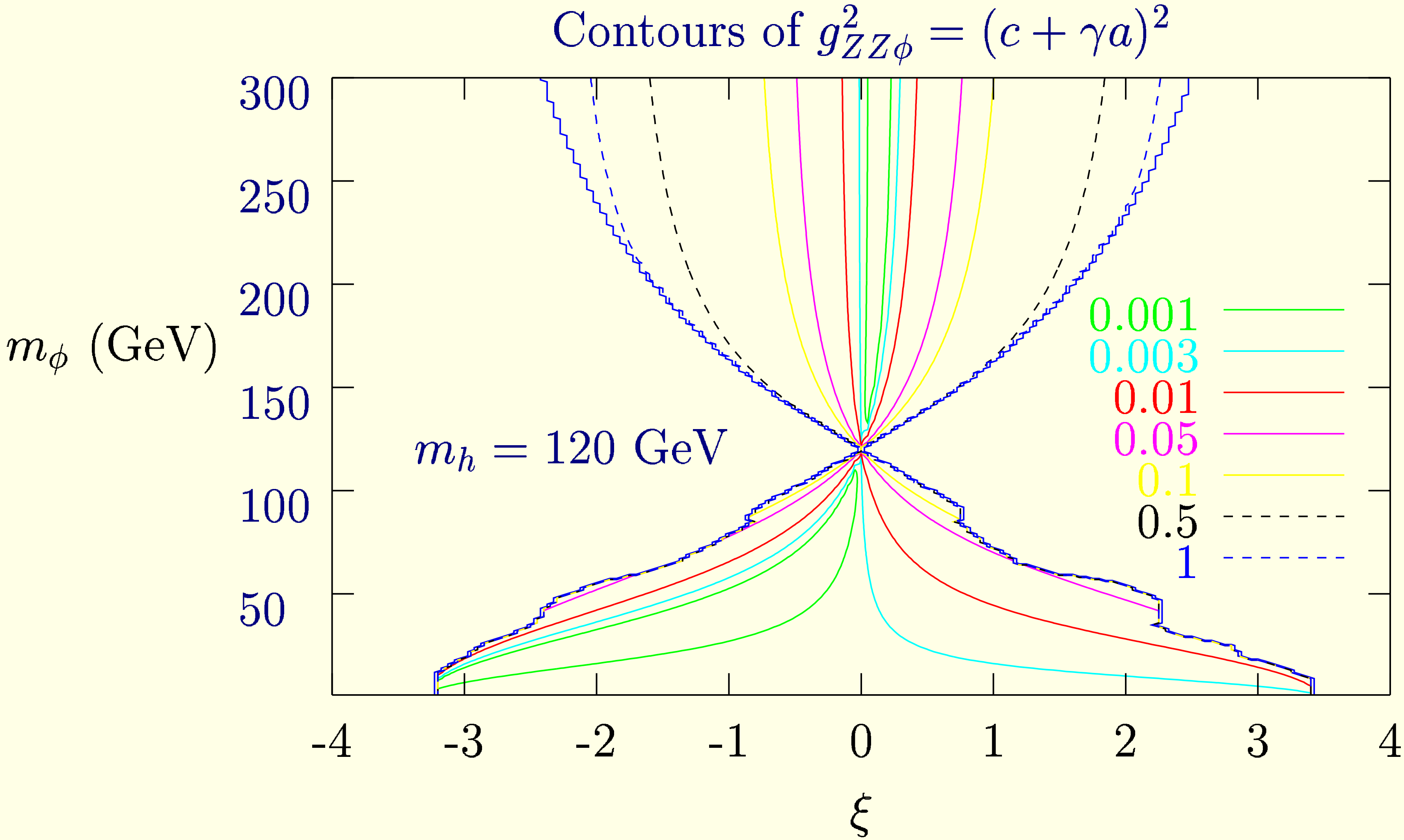

Figure 2: Contours of $g^2_{fV\phi}$ for $\Lambda_\phi = 5$ TeV, $m_h = 120$ GeV

- **Substantial $g^2_{fV\phi}$ is possible if $m_\phi > m_h$ and ξ is not too small.**

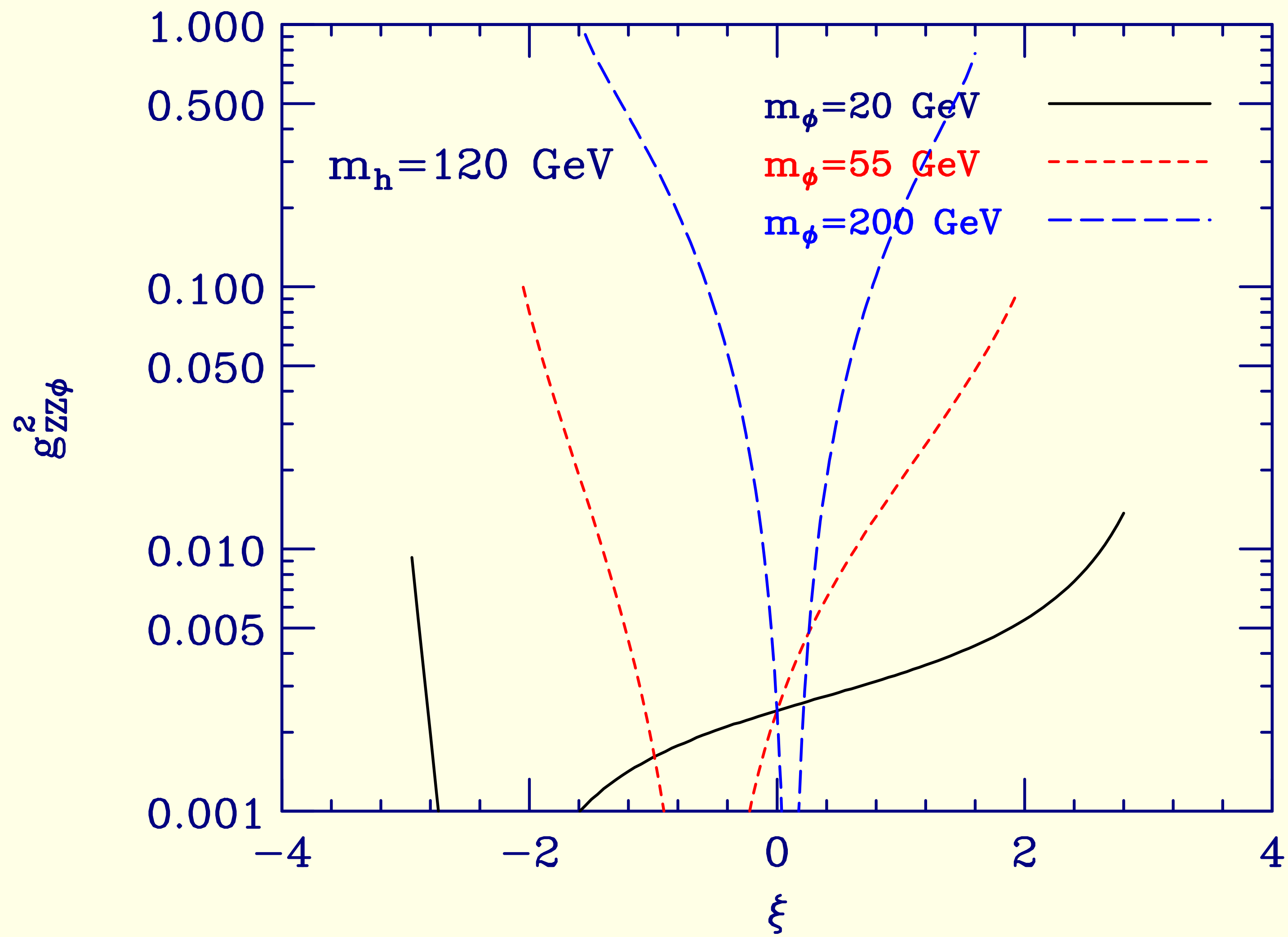

1.000
0.500
0.100
0.050
0.010
0.005
0.001
−4
−2
0
2
4
ξ
$g^2_{ZZ\phi}$
m_h=120 GeV
m_ϕ=20 GeV
m_ϕ=55 GeV
m_ϕ=200 GeV

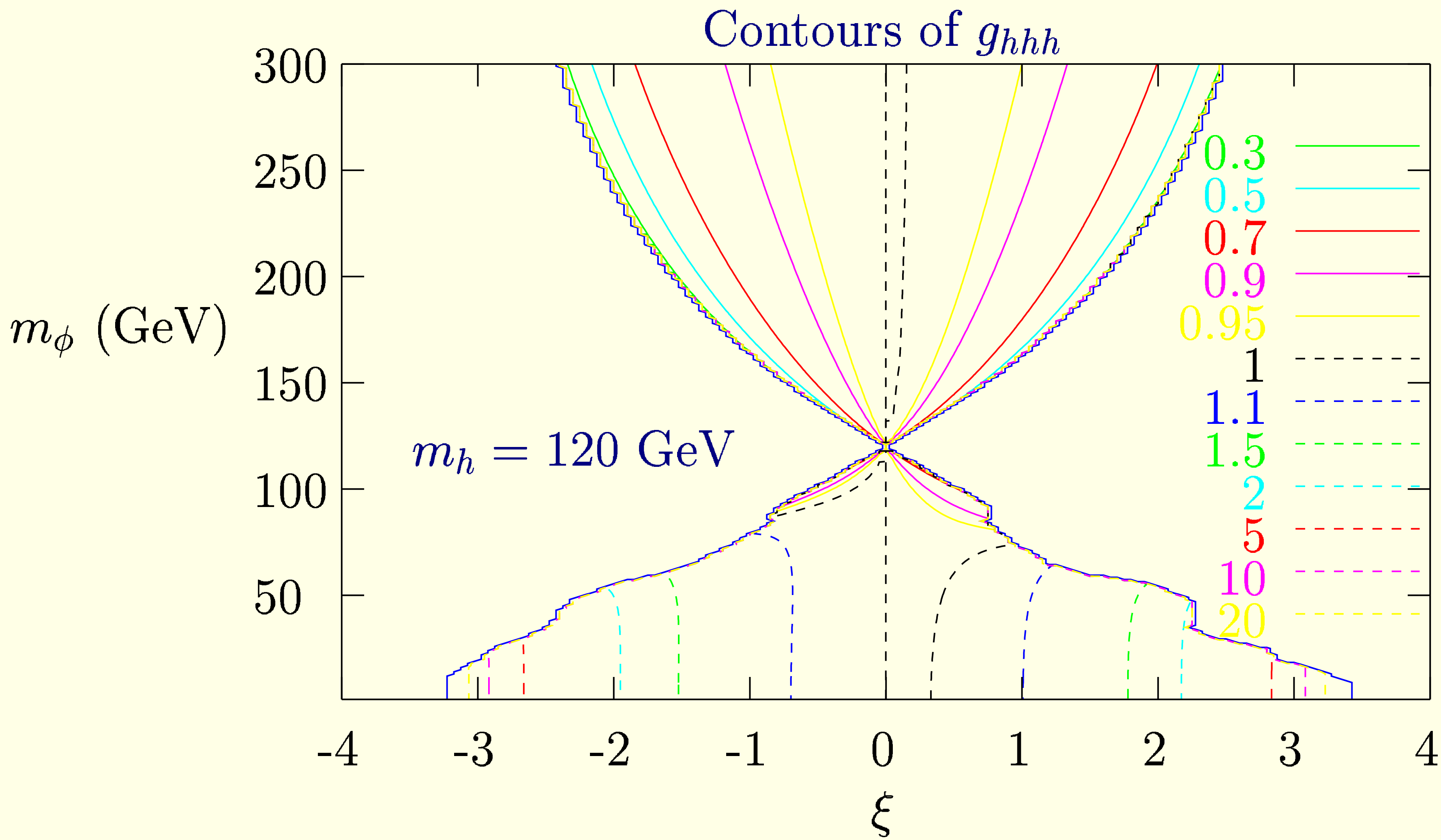

Figure 3: Contours of g_{hhh} relative to the SM for $\Lambda_\phi = 5$ TeV, $m_h = 120$ GeV

- **Once g^2_{fVh} has been measured, g_{hhh} is more or less determined. Consistency of the two is an important check of the model.**

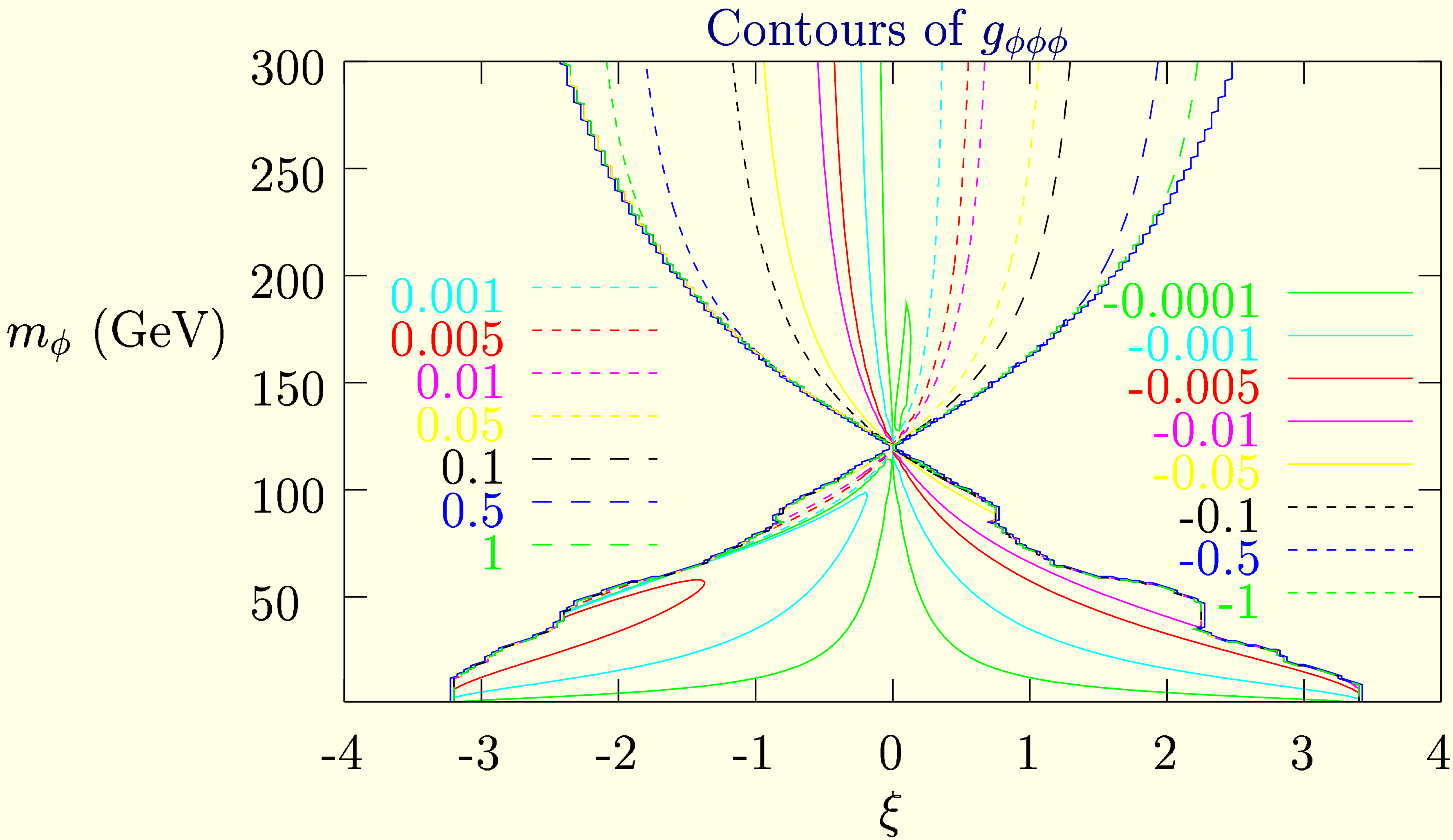

Figure 4: Contours of $g_{\phi\phi\phi}$ relative to the SM for $\Lambda_\phi = 5$ TeV, $m_h = 120$ GeV

- **Substantial values are possible if $m_\phi > m_h$ and ξ is not too small.**

Branching Ratios

Some important points are:

- h branching ratios are quite SM-like (even if partial widths are different) except that $h \to gg$ can be bigger than normal, especially when g_{fVh}^2 is suppressed.
- For $m_\phi < 2m_W$, $\phi \to gg$ is very possibly the dominant mode in the substantial regions near zeroes of $g_{fV\phi}^2$.

  For $m_\phi > 2m_W$, ϕ branching ratios are sort of SM-like (except at $\xi \simeq 0$) but total and partial widths are rescaled.

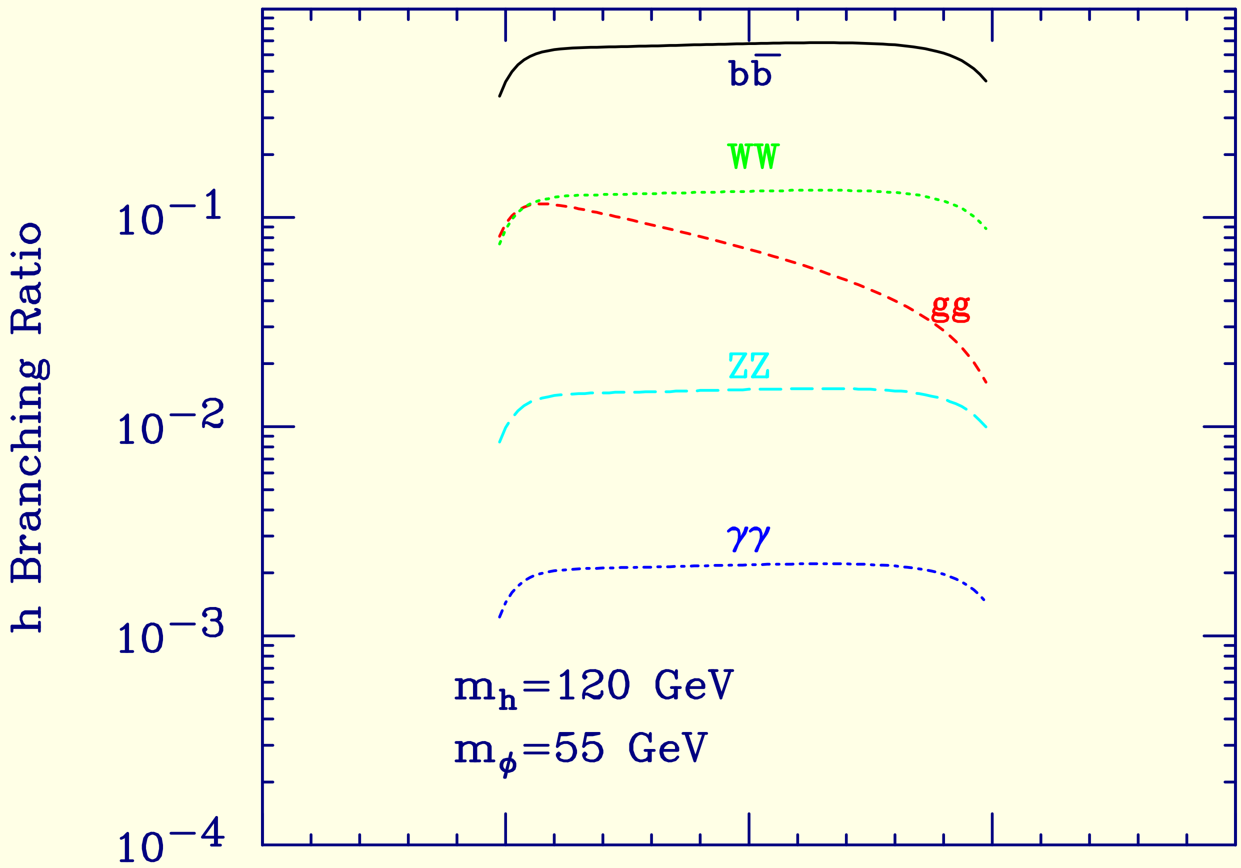
h Branching Ratio
10^{-1}
10^{-2}
10^{-3}
10^{-4}
$b\overline{b}$
WW
gg
ZZ
$\gamma\gamma$
m_h=120 GeV
m_ϕ=55 GeV

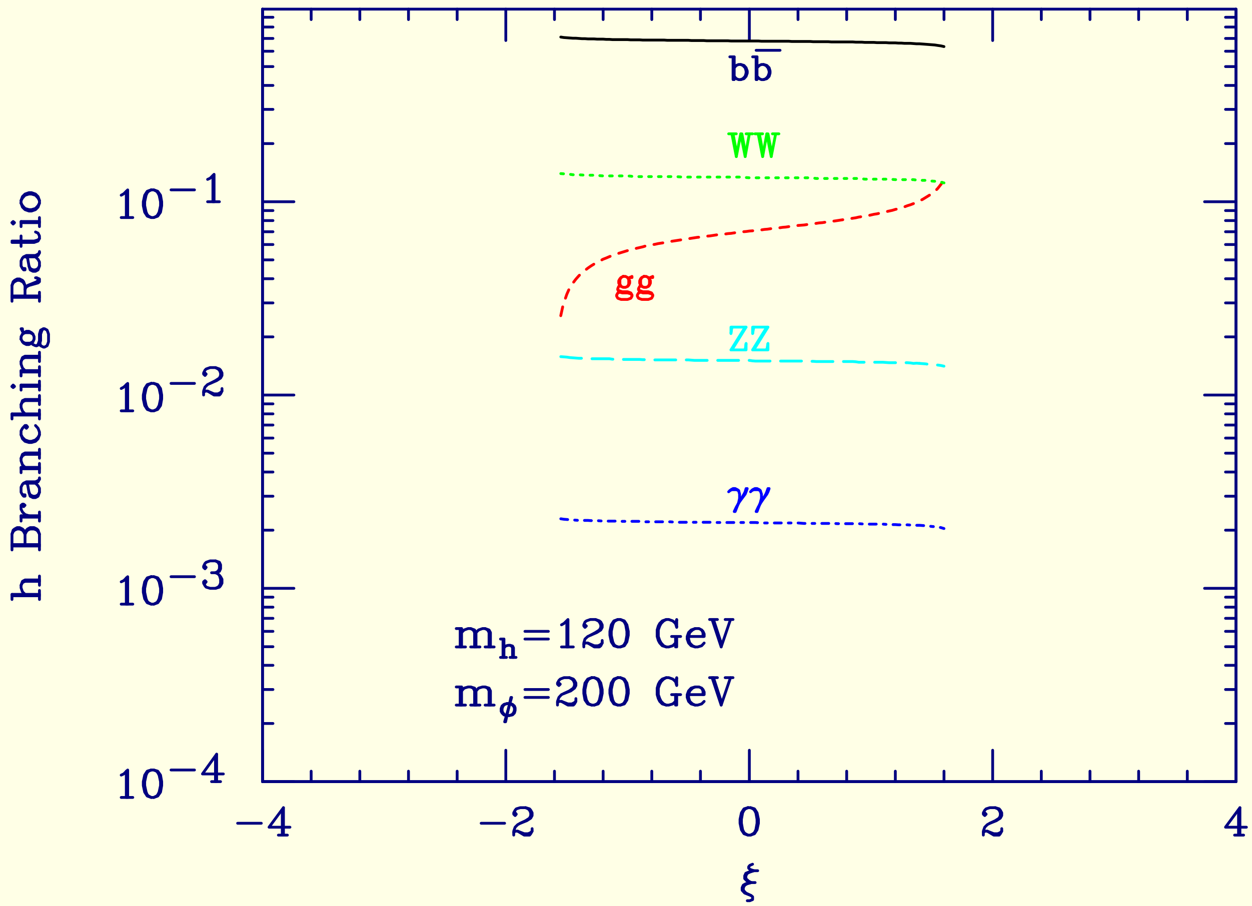
h Branching Ratio
10^{-1}
10^{-2}
10^{-3}
10^{-4}
−4
−2
0
2
4
ξ
$b\bar{b}$
WW
gg
ZZ
$\gamma\gamma$
m_h=120 GeV
m_ϕ=200 GeV

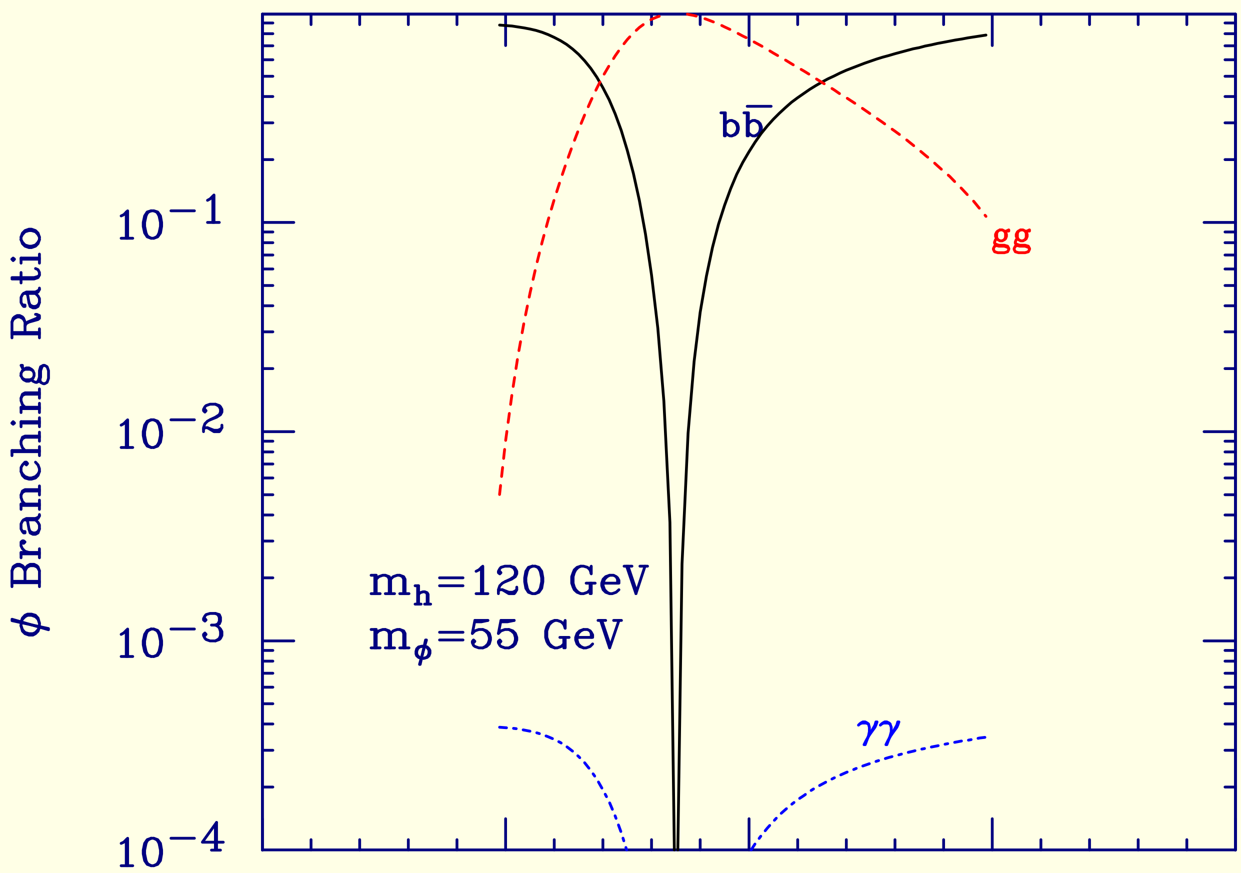

ϕ Branching Ratio
10^{-1}
10^{-2}
10^{-3}
10^{-4}
$b\bar{b}$
gg
$\gamma\gamma$
m_h=120 GeV
m_ϕ=55 GeV

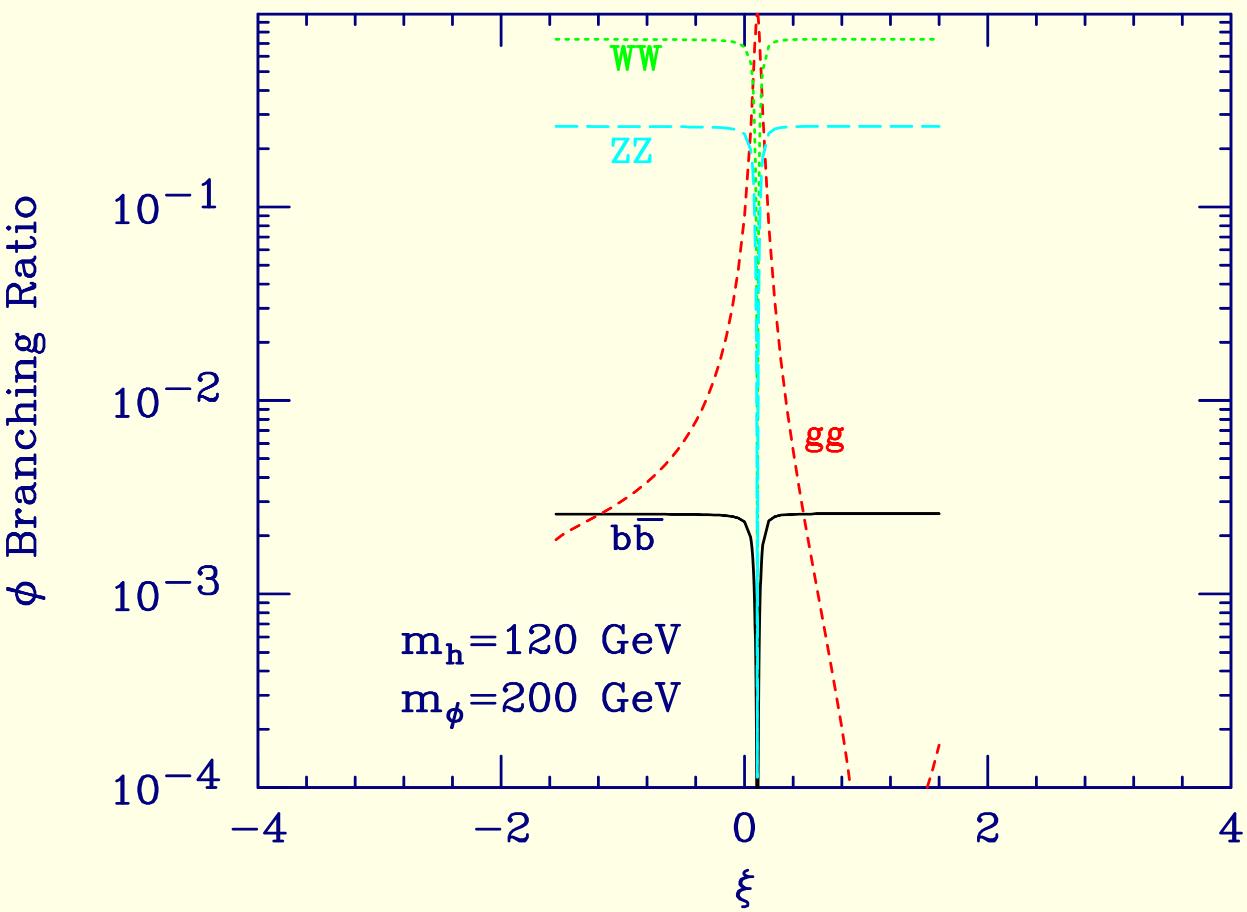
WW
ZZ
gg
$b\bar{b}$
m_h=120 GeV
m_ϕ=200 GeV
ϕ Branching Ratio
ξ
10^{-1}
10^{-2}
10^{-3}
10^{-4}
−4
−2
0
2
4

Strategies

- Ultimately, we would like to use different sources of information on precision h measurements to determine m_ϕ indirectly, and test this indirect determination by direct observation of the ϕ.

- The coincidence of g^2_{fVh}, as measured using VV couplings and $f\overline{f}$ couplings, is a check of the radion theory but fails to determine m_ϕ using only h measurements.

- As we shall shortly discuss, the $gg \to h \to \gamma\gamma$ rate (or the reverse) will provide a crucial piece of information by virtue of the fact that there is a large anomalous contribution to this coupling that is not controlled by g^2_{fVh}.

- However, we will still not know from these h measurements alone what the value of m_ϕ is.

  In some cases, the ϕ will be easily observed, but in other cases not.

- Given an observation of the h and measurement of g^2_{ZZh}, we will have a good idea of whether we should or should not see the ϕ. In particular, if $g^2_{fVh} < 1$ the R^2 sumrule, gives a lower bound of $g^2_{fV\phi} \geq 1 - g^2_{fVh}$.

Note:

Preknowledge of m_ϕ might be crucial for $\gamma\gamma$ observation of the ϕ since the ϕ couplings can be suppressed, implying that we must know how to preset the $W_{\gamma\gamma}$ spectrum peak to be in the vicinity of m_ϕ.

Special Case:

- We will examine one case in detail.

  We assume $m_h = 120~\mathrm{GeV}$ and $g^2_{fVh} = 0.7$.

  $\Rightarrow g^2_{fV\phi} \geq 0.3$ and $m_\phi > 120~\mathrm{GeV}$.

  $\Rightarrow$ the ϕ will be observed if light enough to easily satisfy precision electroweak constraints.

$\boxed{g^2_{fVh} = 0.7}$

- Assume we have detected h at the LHC and at the LC in $e^+e^- \to Zh$ in inclusive recoil and measured g^2_{ZZh} with precision. m_h will be very precisely measured.

  $\Rightarrow$ 2 constraints on 4 parameters of the model.

- Since $g^2_{fV\phi} > 0.3$, assume we have detected the ϕ and measured $g^2_{ZZ\phi}$ (i.e. $g^2_{fV\phi}$) precisely and m_ϕ very precisely.

  Look for $(\xi\gamma, \gamma)$ location(s) where m_ϕ and g^2_{fVh} contours cross.

  $\Rightarrow$ for many cases all 4 parameters of the model are determined except for two-fold ambiguity of $\xi > 0$ vs. $\xi < 0$ and possible ambiguity as to which eigenstate is h and which ϕ.

- In the plots of contours in $(\xi\gamma, \gamma)$ parameter space, the $\gamma = v/\Lambda_\phi < 0.1$ (corresponding to $\Lambda_\phi > 2.46~\mathrm{TeV}$) region is most likely to be relevant.

  A combination of constraints from non-detection of KK excitations at the Tevatron and too-large KK contributions to precision electroweak corrections most probably exclude larger γ (lower Λ_ϕ).

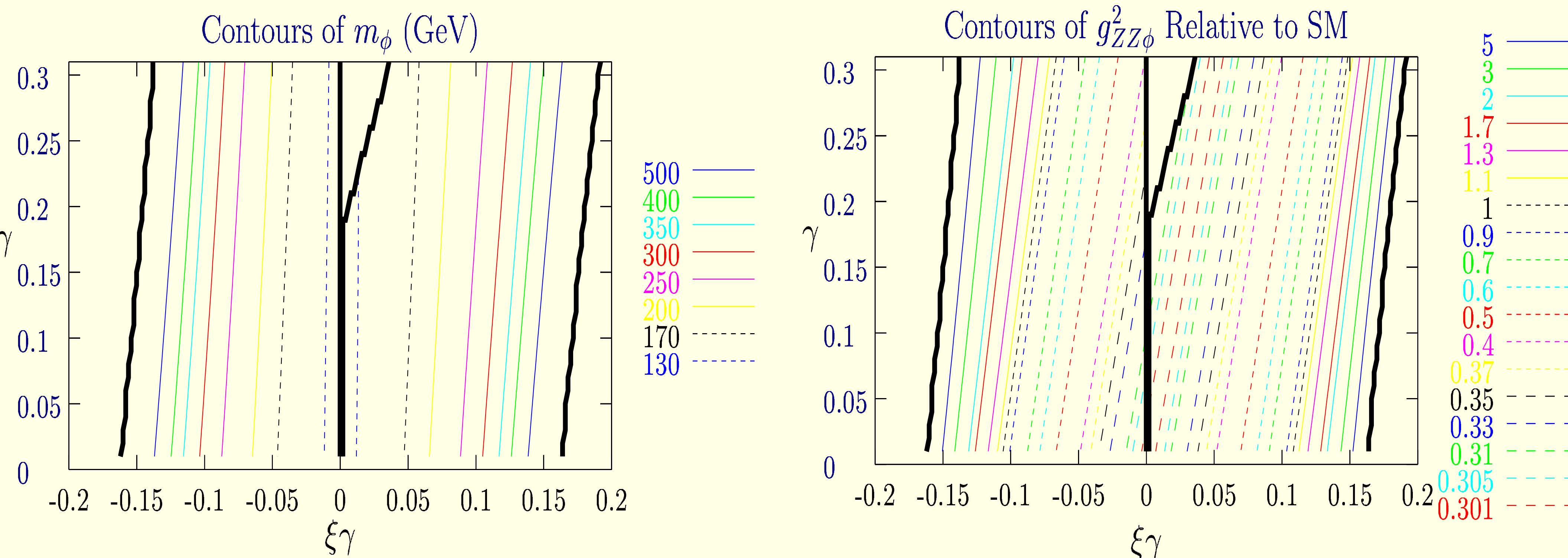

Figure 5: Contours for $m_h = 120$ GeV and $g^2_{fVh} = 0.7$ in $(\xi\gamma, \gamma)$ parameter space.

- **Given the fairly vertical nature of m_ϕ and $g^2_{fV\phi}$ contours, experimental precision on g^2_{fVh} and $g^2_{fV\phi}$ might $\Rightarrow$ uncertainty for $(\xi\gamma, \gamma)$ location(s).**
- **In any case, we will want a way to verify the parameter location and model consistency and to break the $\xi < 0$ vs. $\xi > 0$ and h vs. ϕ ambiguities.**
- **The additional processes of greatest interest are:**
  - $gg \to h \to \gamma\gamma$ **and** $\gamma\gamma \to h \to b\bar{b}$**;**
  - $gg \to \phi \to \gamma\gamma$ **or** ZZ **and** $\gamma\gamma \to \phi \to b\bar{b}$ **or** ZZ **(depending upon** m_ϕ**).**

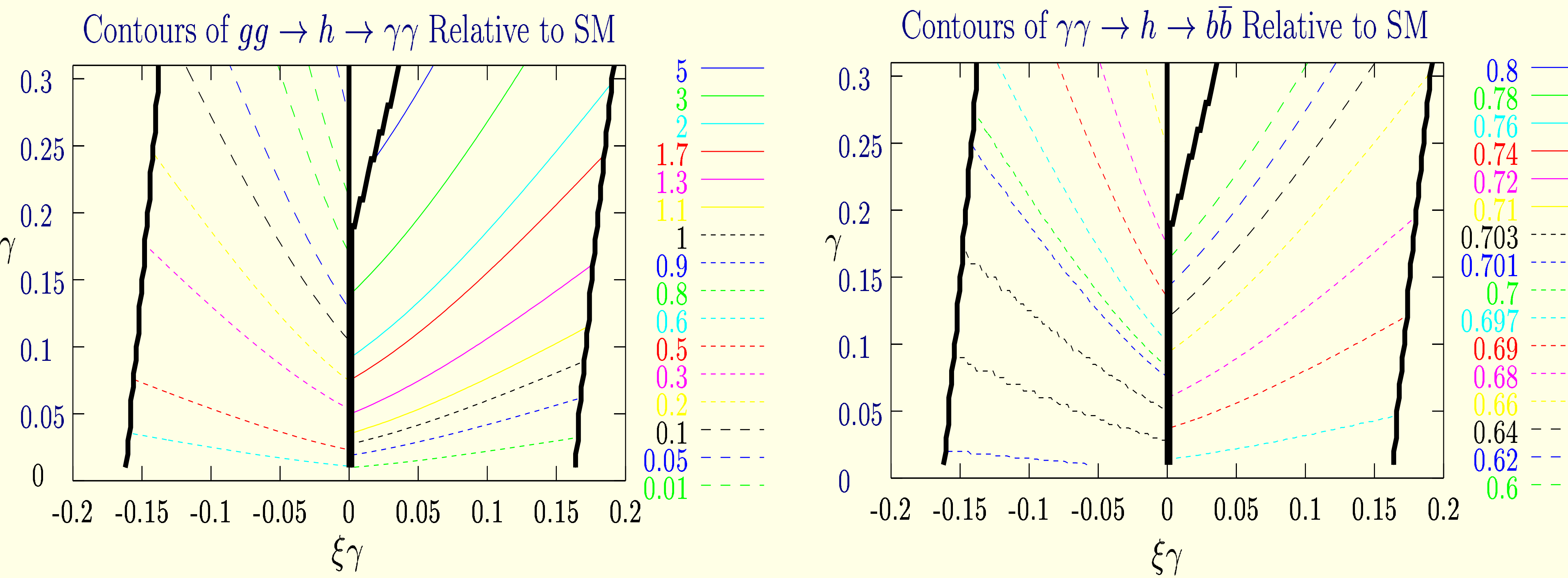

Figure 6: **Contours for $m_h = 120$ GeV and $g^2_{fVh} = 0.7$ in $(\xi\gamma, \gamma)$ parameter space.**

- **The $\gamma\gamma \to h \to b\bar{b}$ rate relative to SM is $\sim g^2_{fVh}$. This weak dependence upon parameter space location allows one to decide that it is the $m_h = 120$ GeV state with $g^2_{fVh} = 0.7$ that is indeed the h. (Compare to later results for the ϕ.)**

- **The $gg \to h \to \gamma\gamma$ rate shows a lot of variation $\Rightarrow$ exact location in parameter space (contours are 'perpendicular' to m_ϕ and $g^2_{fV\phi}$ contours). It is sufficiently large to be observed when γ is small (as preferred).**

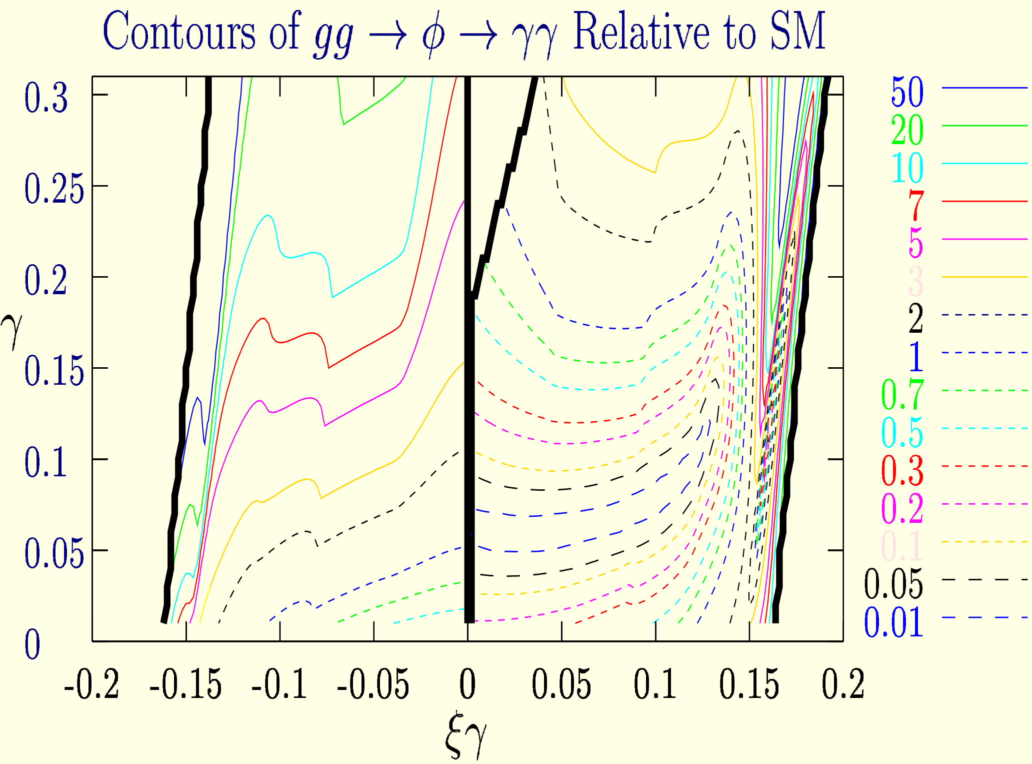

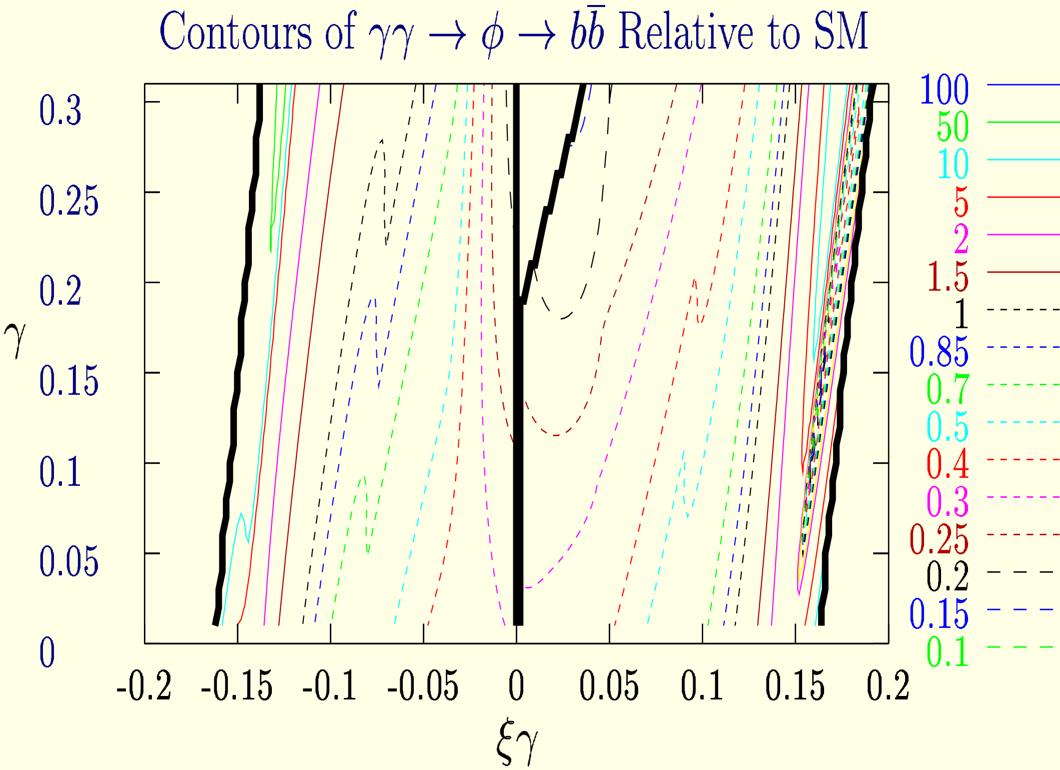

Figure 7: Contours for $m_h = 120$ GeV and $g^2_{fVh} = 0.7$ in $(\xi\gamma, \gamma)$ parameter space.

- **$gg \to \phi \to \gamma\gamma$ is enhanced for $\xi < 0$ and suppressed for $\xi > 0$ (useful to resolve ambiguity).**

  The rate $\Rightarrow$ nice check of anomalous gg coupling of RS model.

- **$\gamma\gamma \to \phi \to b\bar{b}$ is somewhat suppressed for $m_\phi < 300$ GeV, but generally measurable and provides an important check on $\gamma\gamma$ anomalous coupling that is characteristic of RS model.**

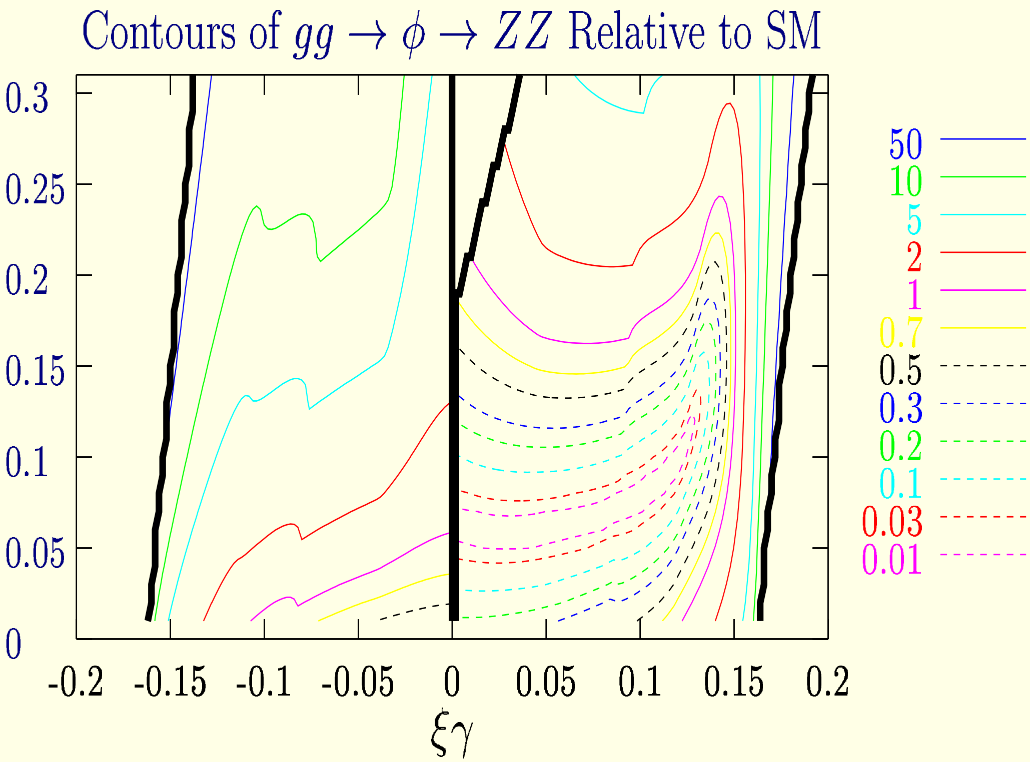

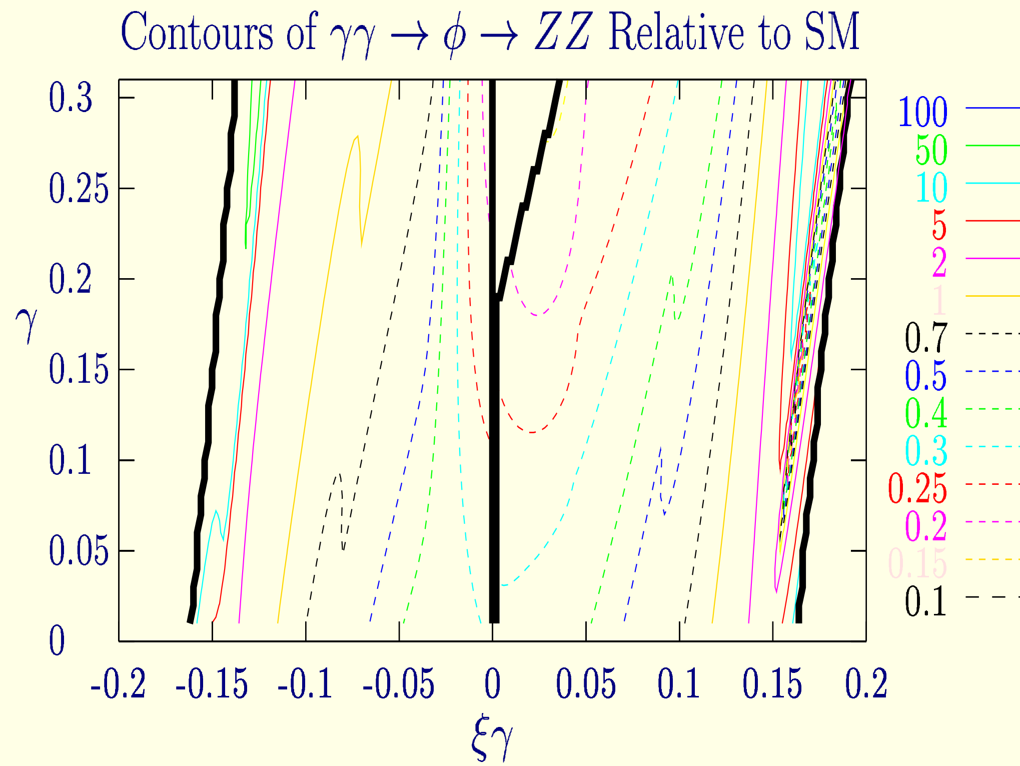

Figure 8: **Contours for $m_h = 120$ GeV and $g^2_{fVh} = 0.7$ in $(\xi\gamma, \gamma)$ parameter space.**

- **The $gg \to \phi \to ZZ$ rate becomes relevant for $m_\phi > 2m_W$.**

  $\Rightarrow$ again a nice check of gg anomalous coupling.

  Where both the $\gamma\gamma$ and ZZ final states can be seen, the rates differ by virtue of anomalous $\gamma\gamma$ coupling — differences tend to be small at small γ.

- **$\gamma\gamma \to \phi \to ZZ$ rate relative to SM is same as for $b\bar{b}$ (it would be nice to check this if $m_\phi \sim 140$ GeV), but only ZZ observable once $m_\phi > 2m_W$.**

- **A final point:**

  Note that there is a certain complementarity between the $gg \to \phi$ rates and the $\gamma\gamma \to \phi$ rates.

  Where the $gg \to \phi \to \gamma\gamma$ and ZZ rates are too suppressed to be detectable ($0 < \gamma\xi < 0.15$, $\gamma \div 0.05 - 0.1$), the $\gamma\gamma \to \phi \to b\bar{b}$ and ZZ rates remain adequate for reasonably precise measurement.

Determining the anomalous gg and $\gamma\gamma$ coupling.

- The first question is what fraction of the gg and $\gamma\gamma$ couplings of the h (and ϕ eventually also) is due to the anomalous coupling components.

  This is illustrated in the first two figures. They show the ratios R_{hgg}, $R_{\phi gg}$, $R_{h\gamma\gamma}$ and $R_{\phi\gamma\gamma}$ defined as

$$R_{hgg} = \frac{g_{ggh}^2(\text{with anomaly})}{g_{ggh}^2(\text{without anomaly})}, \quad \ldots \tag{19}$$

- We will observe that this fraction is substantial in the gg case, but very small in the $\gamma\gamma$ case.

- An important goal would be to establish firmly (i.e. in a model-independent manner) the presence of the anomalous component of the $gg \to h$ coupling.

  This requires the $\gamma\gamma$ collider, as I will discuss in a moment.

Figure 9: R_{hgg} **and** $R_{\phi gg}$ **for** $\Lambda_\phi = 5$ TeV, $m_h = 120$ GeV

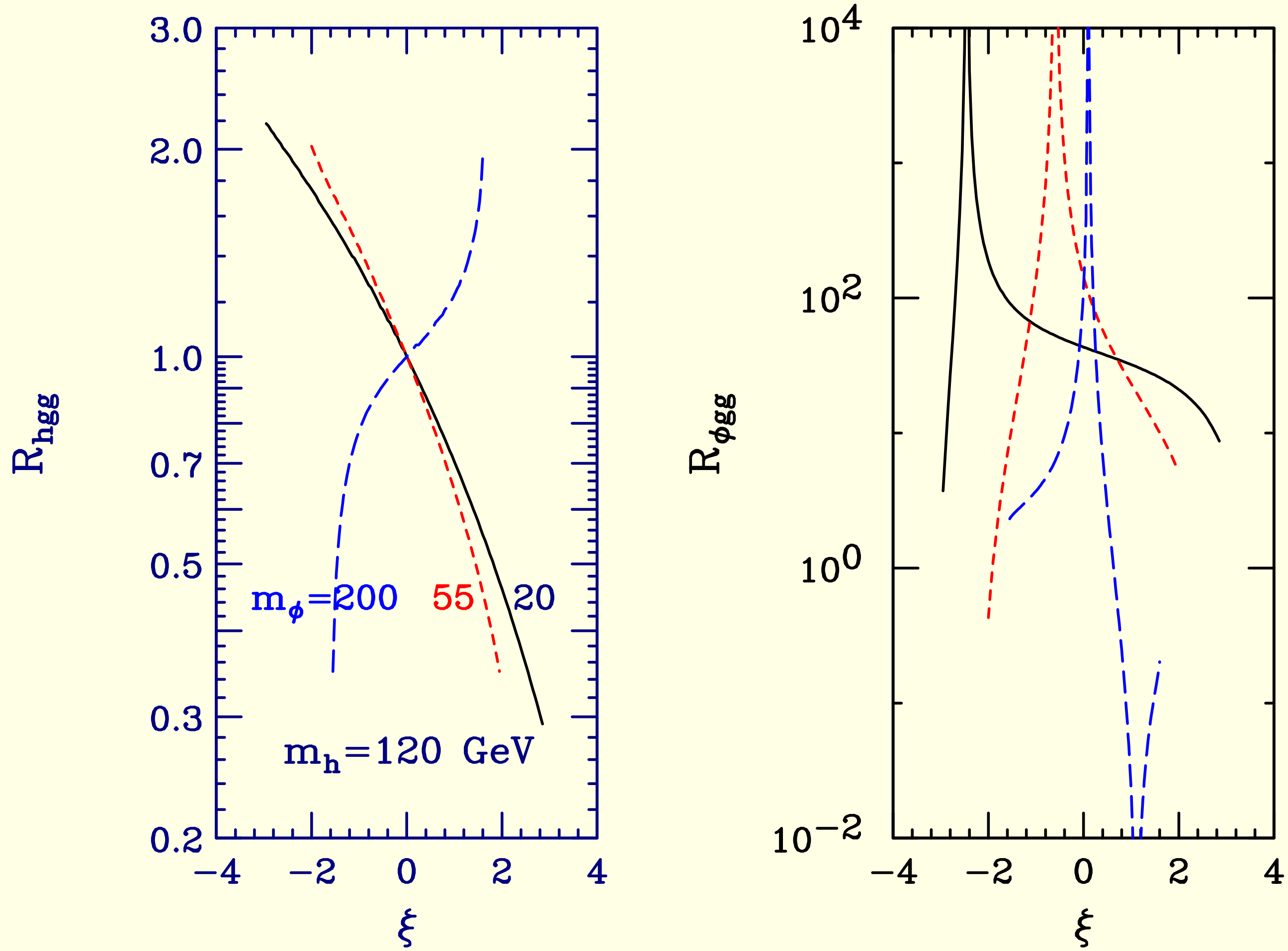

Figure 10: $R_{h\gamma\gamma}$ and $R_{\phi\gamma\gamma}$ for $\Lambda_\phi = 5$ TeV, $m_h = 120$ GeV

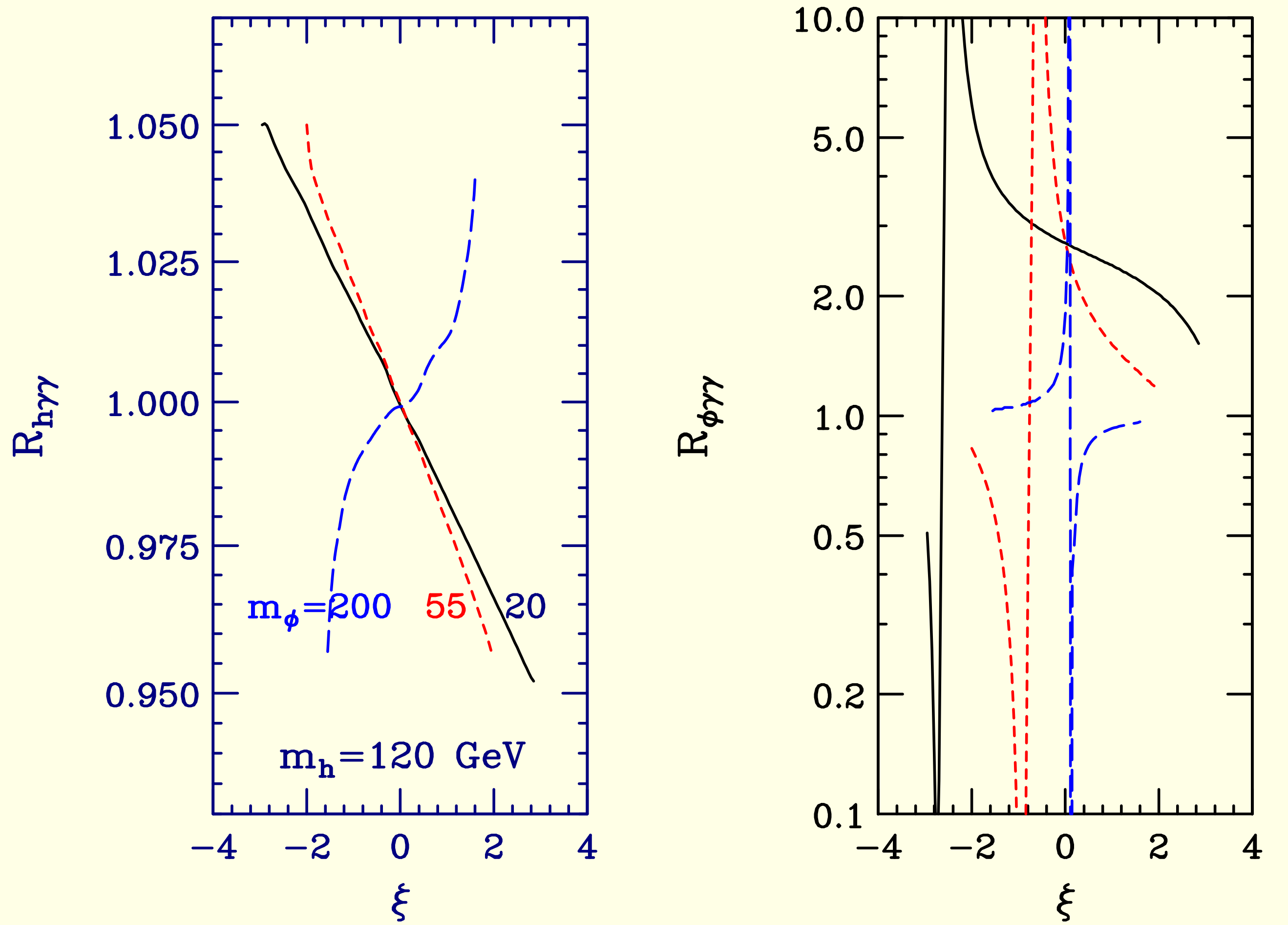

Determination of R_{sgg} and $R_{s\gamma\gamma}$, $s = h, \phi$

First, (model-independent) measurements of the $g^2_{fVh} = (d + \gamma b)^2$ and $g^2_{fV\phi} = (c + \gamma a)^2$ coupling factors for the h and ϕ are obtained using $e^+e^- \to Zh$ and $e^+e^- \to Z\phi$ production at the linear collider. The sgg and $s\gamma\gamma$ couplings ($s = h$ or ϕ) expected from the standard fermion and W-boson loops in the absence of the anomalous contribution can then be computed.

Meanwhile, the actual couplings-squared, g^2_{sgg} and $g^2_{s\gamma\gamma}$, including any anomalous contribution, can be directly measured using a combination of $\gamma\gamma \to s \to b\overline{b}$ and $gg \to s \to \gamma\gamma$ data.

In more detail, we employ the following procedures (for m_s such that $b\overline{b}$ decay is primary).

- First, obtain g^2_{ZZs} (defined relative to the SM prediction at $m_{h_{\rm SM}} = m_s$) from $\sigma(e^+e^- \to Zs)$ (inclusive recoil technique).
- Next, determine $BR(s \to b\overline{b}) = \sigma(e^+e^- \to Zs \to Zb\overline{b})/\sigma(e^+e^- \to Zs)$.
- Then, compute $g^2_{s\gamma\gamma}$ from $\sigma(\gamma\gamma \to s \to b\overline{b})/BR(s \to b\overline{b})$.
- To display the contribution to the $s\gamma\gamma$ coupling-squared from the anomaly

one would then compute

$$R_{s\gamma\gamma} \equiv \frac{g^2_{s\gamma\gamma}(\text{from experiment})}{g^2_{h_{\rm SM}\gamma\gamma}(\text{as computed for } m_{h_{\rm SM}} = m_s) \times g^2_{ZZs}(\text{from experiment})} \tag{20}$$

- To determine g^2_{sgg} experimentally requires one more step. We must compute $\sigma(gg \to s \to \gamma\gamma)/BR(s \to \gamma\gamma)$. To obtain $BR(s \to \gamma\gamma)$, we need a measurement of $\Gamma^{\rm tot}_s$.

  Given such a measurement, we then compute

$$BR(s \to \gamma\gamma) = \frac{\Gamma(s \to \gamma\gamma)(\text{computed from } g^2_{s\gamma\gamma})}{\Gamma^{\rm tot}_s(\text{from experiment})}, \tag{21}$$

  where the above experimental determination of $g^2_{s\gamma\gamma}$ is employed and the experimental techniques outlined in LC TDR's are employed for $\Gamma^{\rm tot}_s$ (for which $\gamma\gamma$ collider input is helpful).

- **The ratio analogous to Eq. (20) for the gg coupling is then**

$$R_{sgg} \equiv \frac{g^2_{sgg}(\text{from experiment})}{g^2_{h_{\rm SM}gg}(\text{as computed for } m_{h_{\rm SM}} = m_s) \times g^2_{ZZs}(\text{from experiment})} \,. \tag{22}$$

For a light SM Higgs boson, the various cross sections and branching ratios needed for the $s\gamma\gamma$ coupling can be determined with errors of order a few percent. A careful study is needed to assess the prospects in various RS scenarios.

$\gamma\gamma \to h, \phi \to \gamma\gamma$?

- The study by M. Schmitt finds that $\gamma\gamma \to h_{\rm SM} \to \gamma\gamma$ is observable for $m_{h_{\rm SM}} \sim 120~{\rm GeV}$.
- What can we learn from the analogous h, ϕ RS predictions?

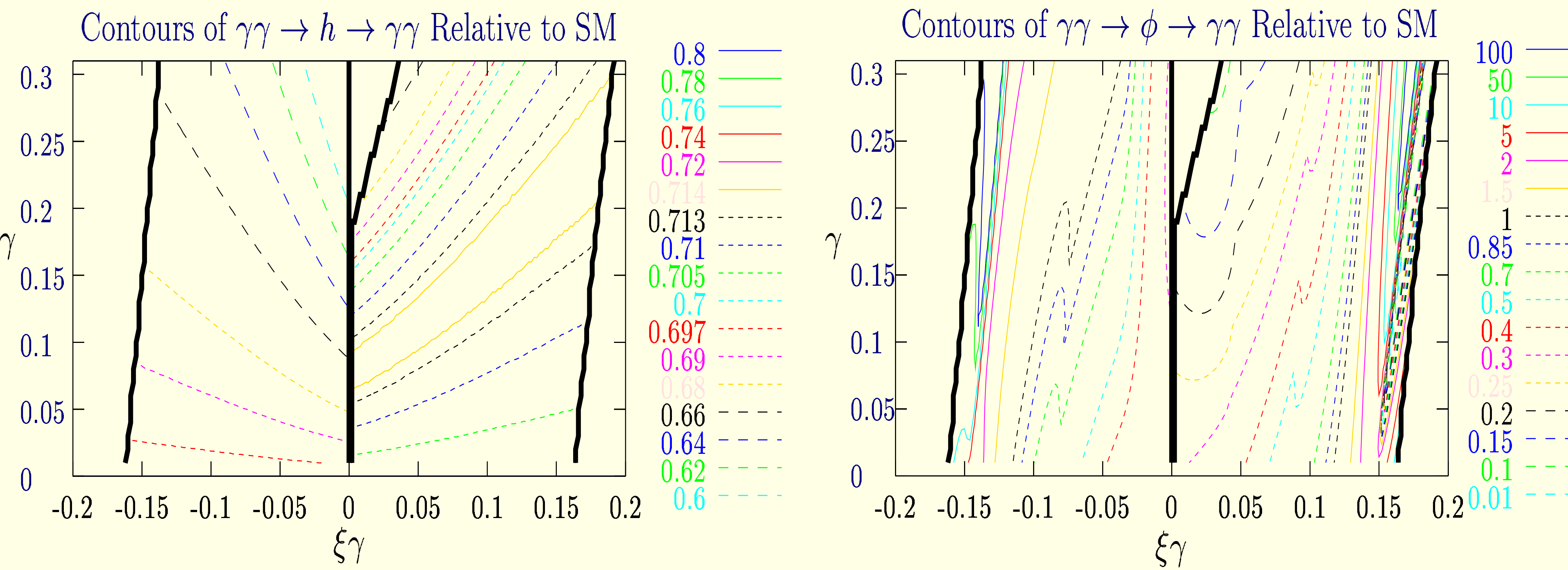

Figure 11: Contours for $m_h = 120~{\rm GeV}$ and $g^2_{fVh} = 0.7$ in $(\xi\gamma, \gamma)$ parameter space.

- The h rate is approximately $g^2_{fVh}\times$SM. ($\Rightarrow$ another check of which state is the h.)

- Still, variation in $(\xi\gamma, \gamma)$ parameter space at the $\sim 10\%$ level is apparent and would allow cross check of $(\xi\gamma, \gamma)$ parameter location, presence of anomalous coupling and model consistency.
- The $\gamma\gamma \to \phi \to \gamma\gamma$ rate shows a lot of variation in the small $|\xi\gamma|$ region where $m_\phi \lesssim 140~\mathrm{GeV}$, *i.e.* for m_ϕ such that $BR(\phi \to \gamma\gamma)$ would be large enough that the rate might be measurable.
- However, for many such parameter points, the suppression relative to the SM comparison rate is sufficiently substantial that the accuracy of the measurement would be relatively poor.
- Still, if other aspects of the RS model are verified, this would be a very interesting final check on the model, especially the magnitude of the anomalous contribution to the $\phi \to \gamma\gamma$ coupling.

  In particular, the ratio of the $\gamma\gamma \to \phi \to \gamma\gamma$ rate relative to the SM comparison differs substantially from the corresponding ratios for $\gamma\gamma \to \phi \to b\overline{b}$ and ZZ (as plotted in earlier) at any given $(\xi\gamma, \gamma)$ parameter location, whereas these ratios would be the same in the absence of the anomalous coupling.

CONCLUSIONS

- The Higgs-radion sector will certainly be very revealing.

  For some parameter choices it may prove quite easy to fully explore. For others, somewhat difficult.

- In fact, at the LHC one can miss both the ϕ and the h for the most difficult parameter choices.

  The LC would be crucial in such a case.

- Even for the kind of case detailed here where both h and ϕ can be easily seen at the LHC, the LC will play a vital role and beautifully complement the LHC data.

- In particular, large deviations of h properties with respect to $h_{\rm SM}$ properties are typically expected and the ϕ will display even greater differences.

  To fully interpret, need the combination of LHC and LC data.

- **The $\gamma\gamma$ collider will play a crucial role in verifying the predicted structure of the anomalous gg and $\gamma\gamma$ couplings.**

- **We have focused on scenarios where $h \to \phi\phi$ or $h \to h^n\phi$ decays are not important ($m_\phi > m_h$), but if $m_\phi \lesssim m_h/2$ they can be quite important.**

  Built into our results for $m_\phi > 2m_h$ are $\phi \to hh$ decays, that become quite important once $m_\phi \geq 300~\mathrm{GeV}$ when $m_h = 120~\mathrm{GeV}$. But, for $g^2_{fV\phi} > 0.3$, it is probable that such large m_ϕ values are inconsistent with precision electroweak data.